Prior Art Model

ALTERNATIVE SPLICED EXONS	NO. OF AMINO ACIDS ENCODED
α	21
β	37
γ	38

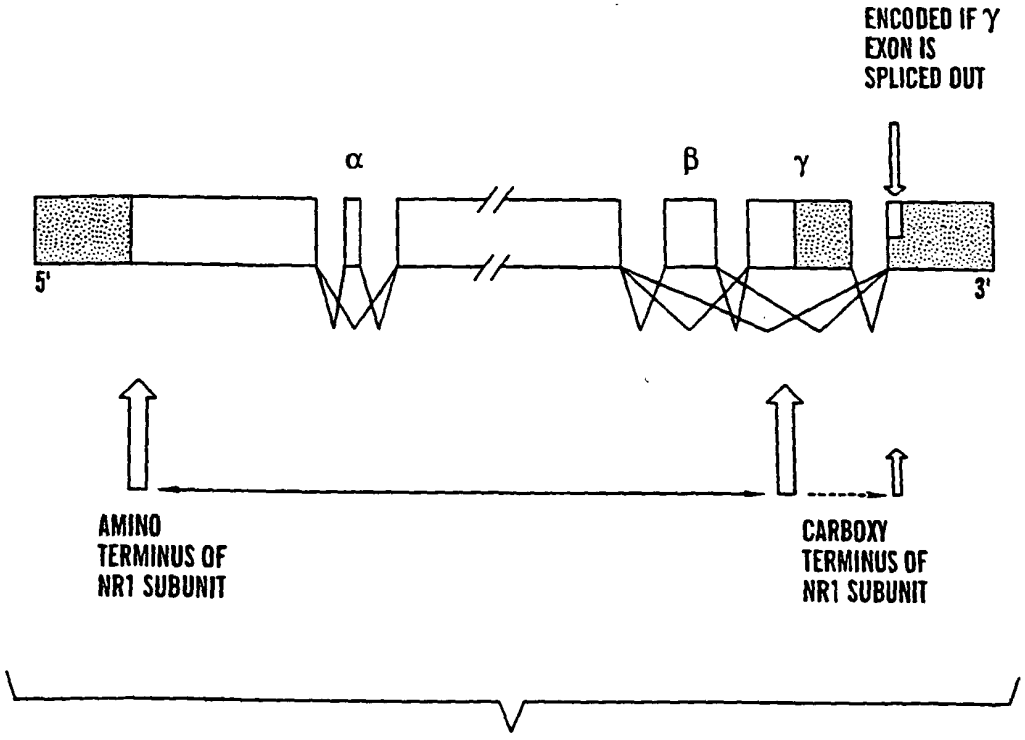

FIG. 1

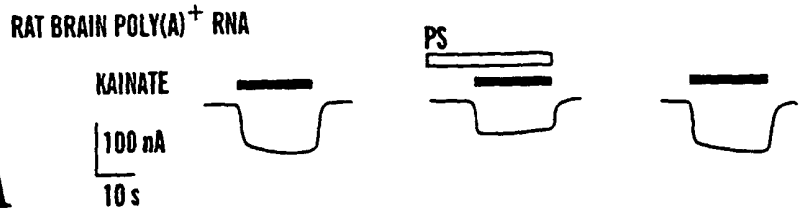

FIG. 2A

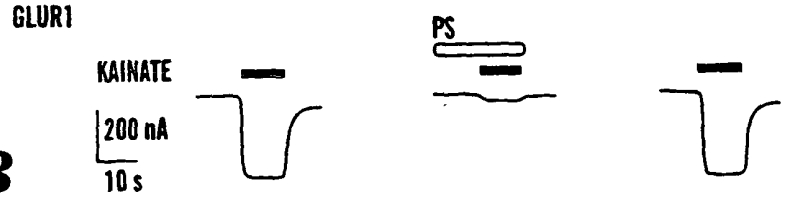

FIG. 2B

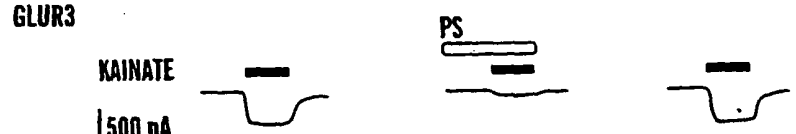

FIG. 2C

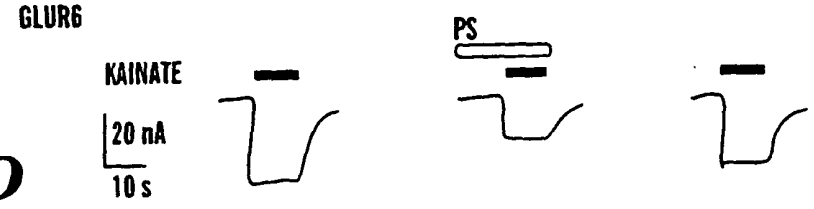

FIG. 2D

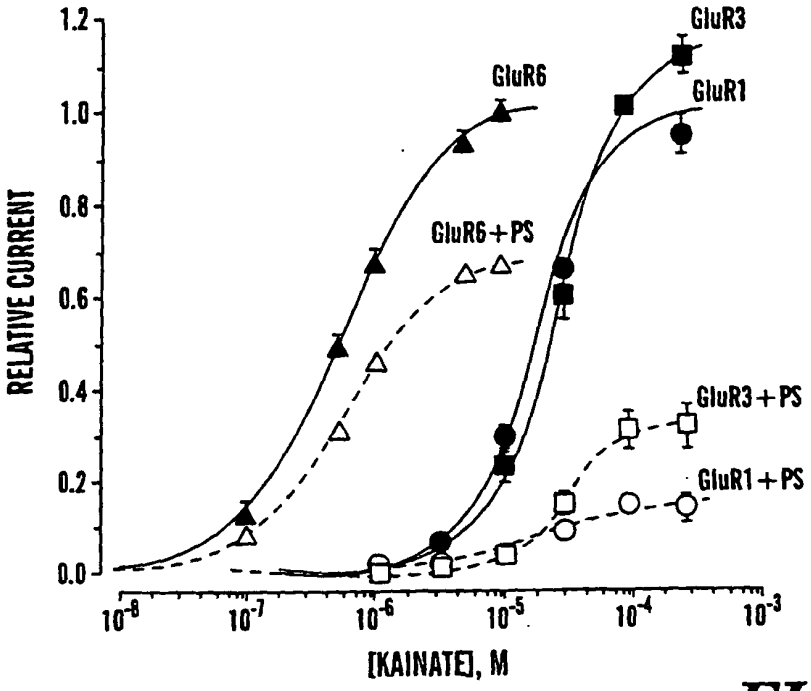
RELATIVE CURRENT
1.2
1.0
0.8
0.6
0.4
0.2
0.0
GluR3
GluR6
GluR1
GluR6+PS
GluR3+PS
GluR1+PS
10^{-8}
10^{-7}
10^{-6}
10^{-5}
10^{-4}
10^{-3}
[KAINATE], M

FIG. 2E

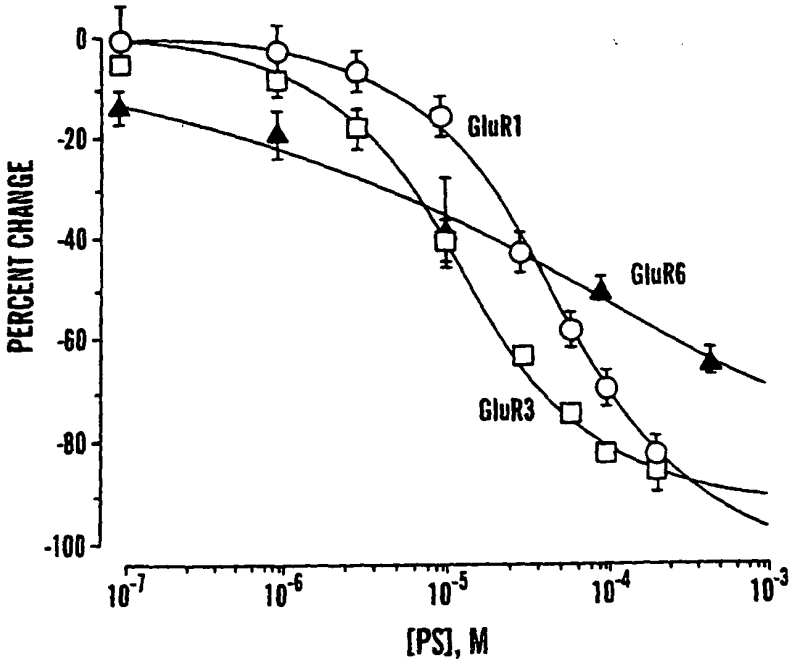
PERCENT CHANGE
0
-20
-40
-60
-80
-100
GluR1
GluR6
GluR3
10^{-7}
10^{-6}
10^{-5}
10^{-4}
10^{-3}
[PS], M

FIG. 2F

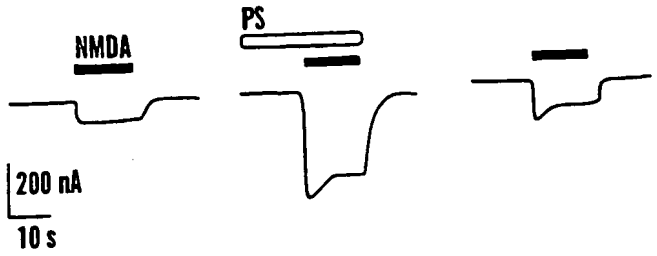

FIG. 3A

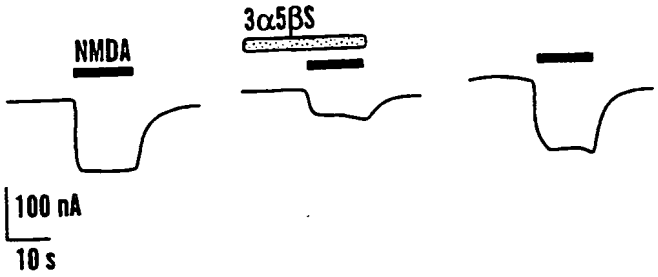

FIG. 3B

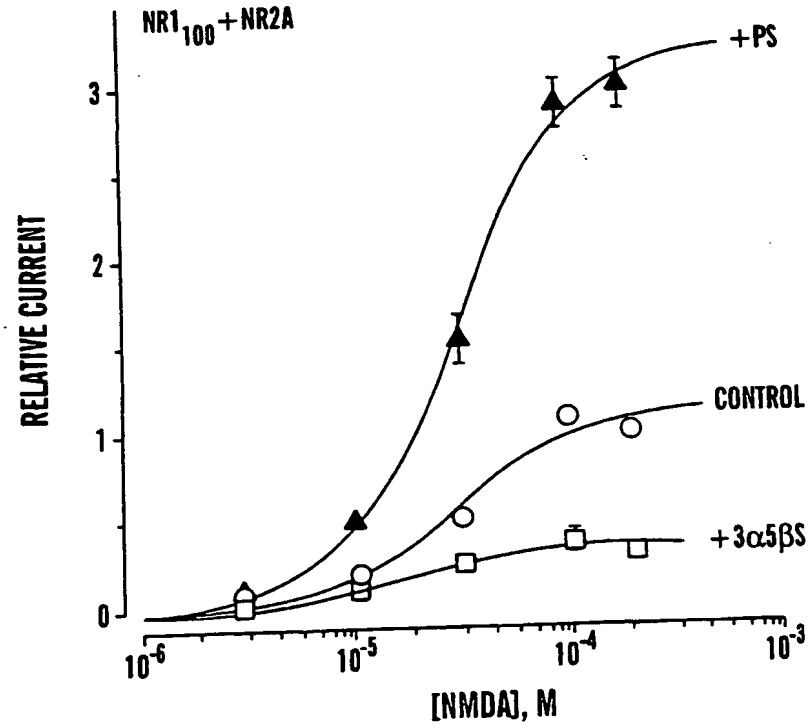

FIG. 3C

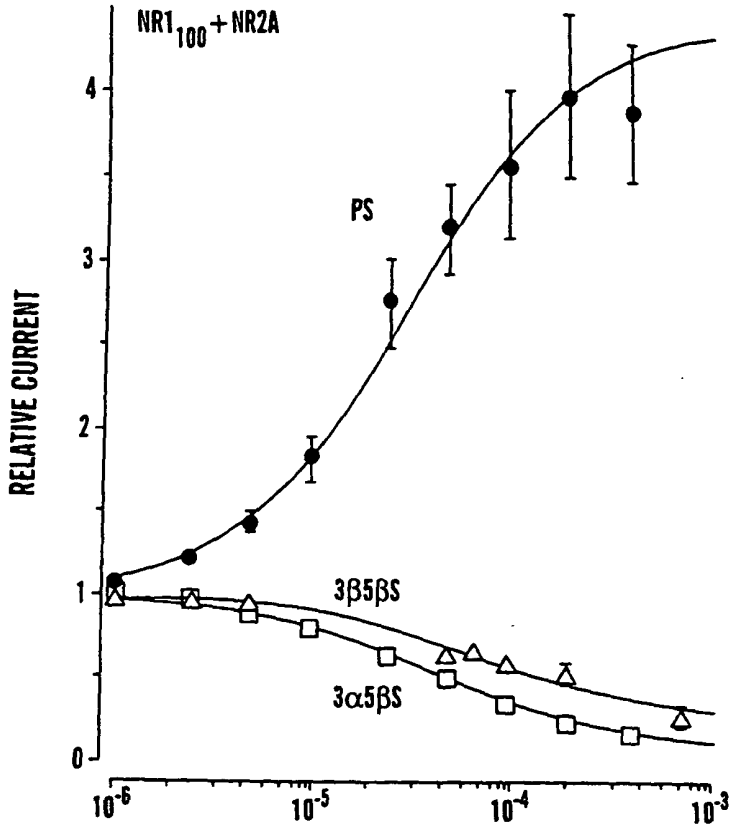
NR1100+NR2A
RELATIVE CURRENT
PS
3β5βS
3α5βS
[STEROID], M

FIG. 3D

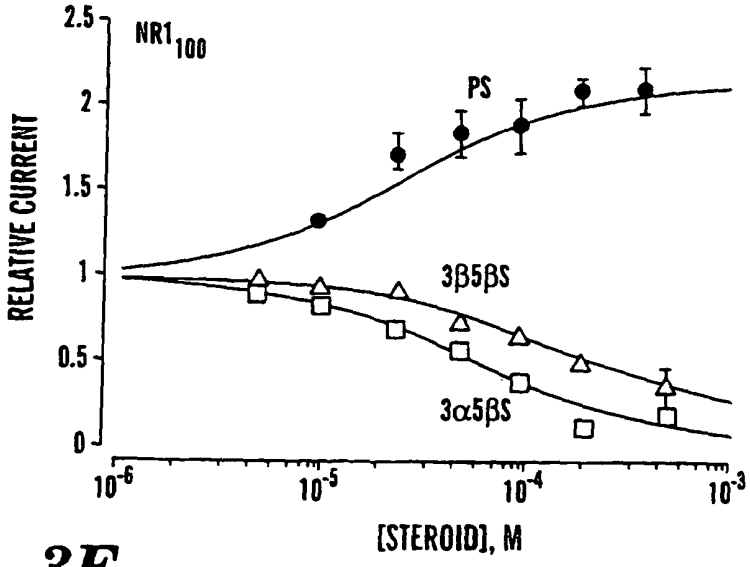
NR1100
RELATIVE CURRENT
PS
3β5βS
3α5βS
[STEROID], M

FIG. 3E

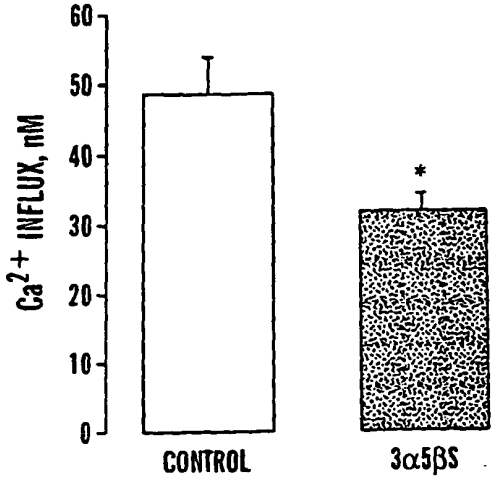
60
50
40
30
20
10
0
Ca^{2+} INFLUX, nM
*
CONTROL
3α5βS

FIG. 4A

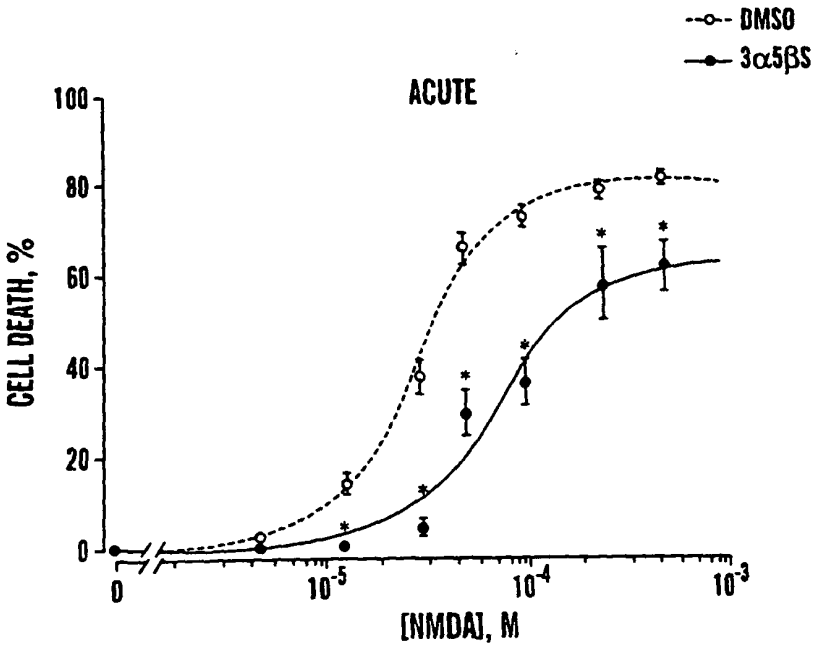
DMSO
3α5βS
ACUTE
100
80
60
40
20
0
CELL DEATH, %
0
10^{-5}
10^{-4}
10^{-3}
[NMDA], M

FIG. 4B

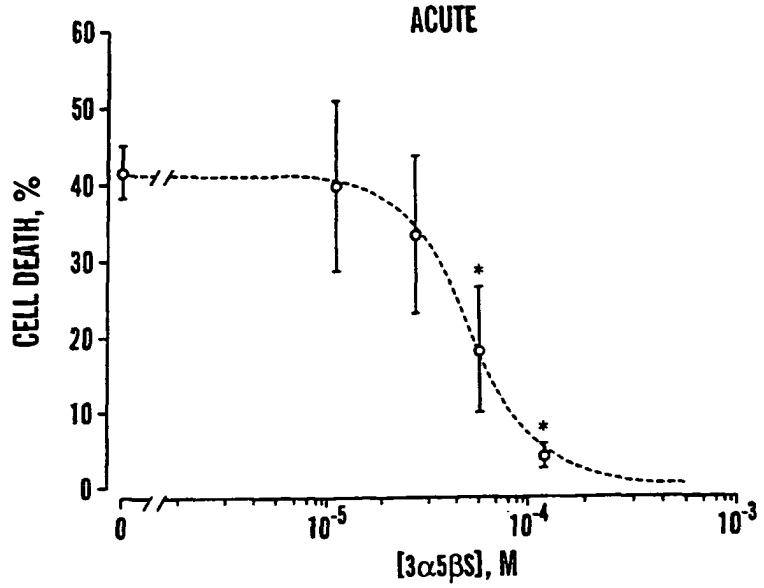
ACUTE
CELL DEATH, %
60
50
40
30
20
10
0
0
10^{-5}
10^{-4}
10^{-3}
[3α5βS], M
*
*

FIG. 4C

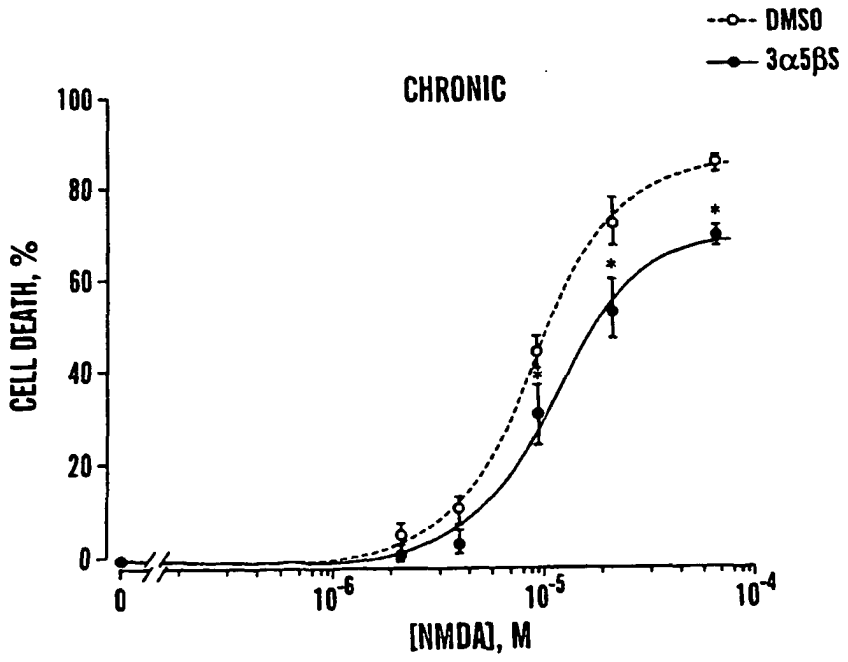
DMSO
3α5βS
CHRONIC
CELL DEATH, %
100
80
60
40
20
0
0
10^{-6}
10^{-5}
10^{-4}
[NMDA], M
*
*
*
*

FIG. 4D

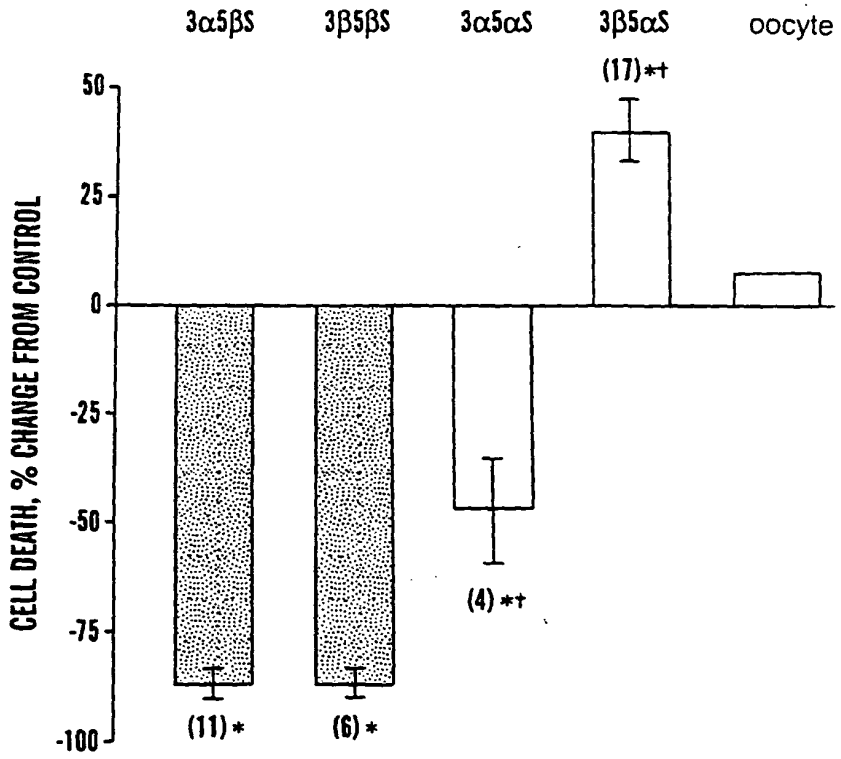
3α5βS
3β5βS
3α5αS
3β5αS
oocyte
(17)*†
50
25
0
-25
-50
-75
-100
CELL DEATH, % CHANGE FROM CONTROL
(4)*†
(11)*
(6)*

FIG. 5

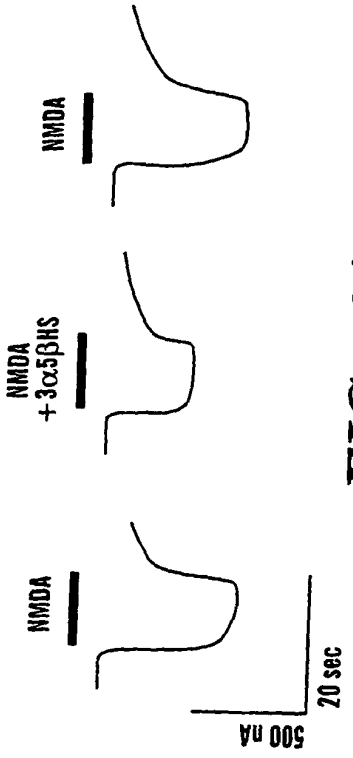

FIG. 6A

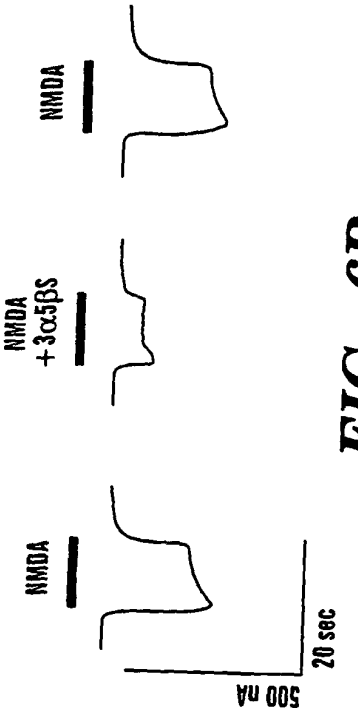

FIG. 6B

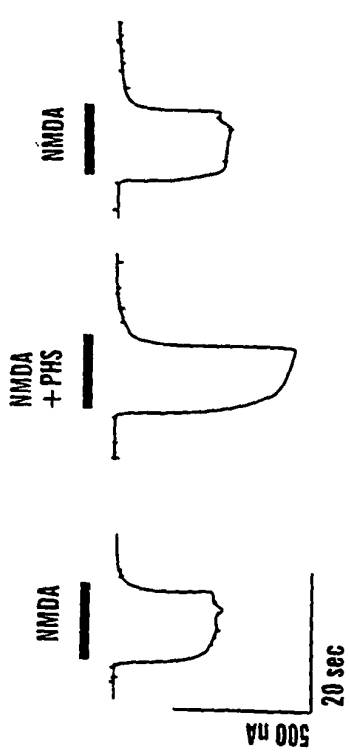

FIG. 6C

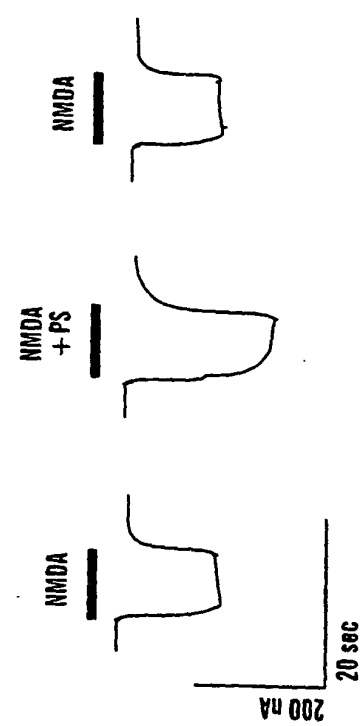

FIG. 6D

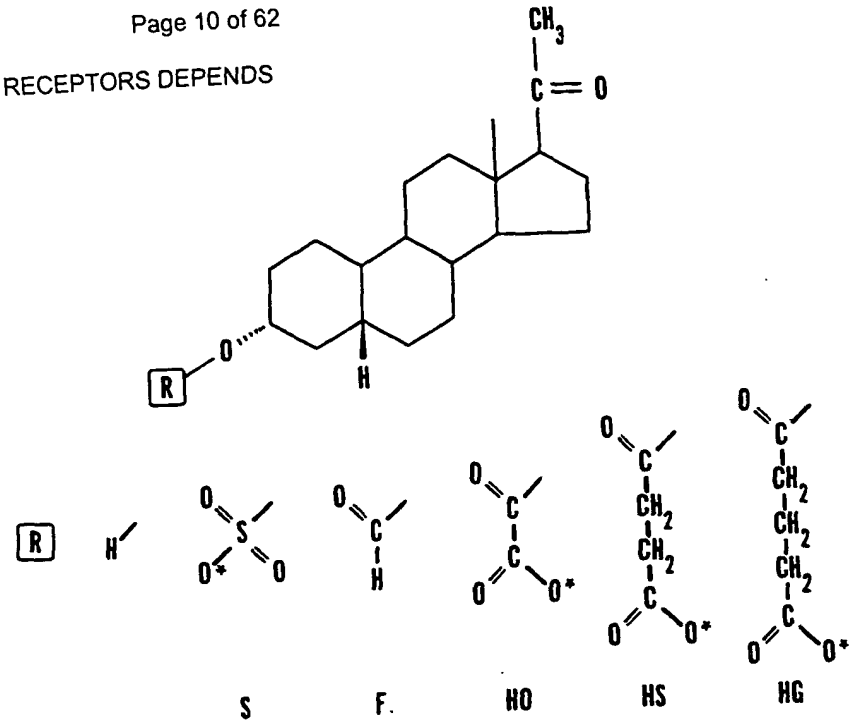
R
H
S
F
HO
HS
HG

FIG. 7A

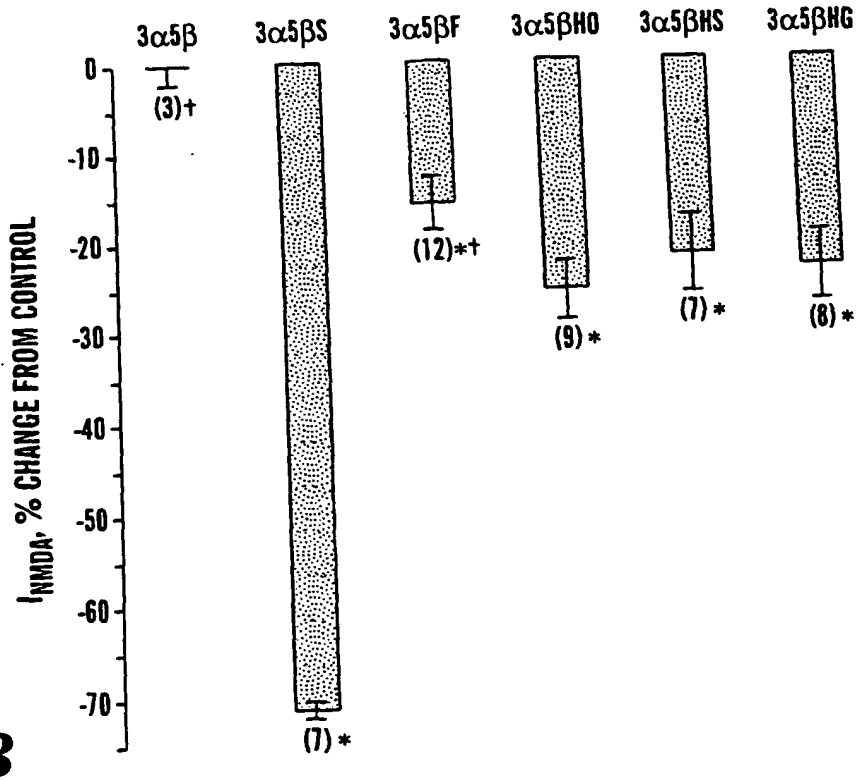
3α5β
3α5βS
3α5βF
3α5βHO
3α5βHS
3α5βHG
0
-10
-20
-30
-40
-50
-60
-70
I_NMDA, % CHANGE FROM CONTROL
(3)†
(7)*
(12)*†
(9)*
(7)*
(8)*

FIG. 7B

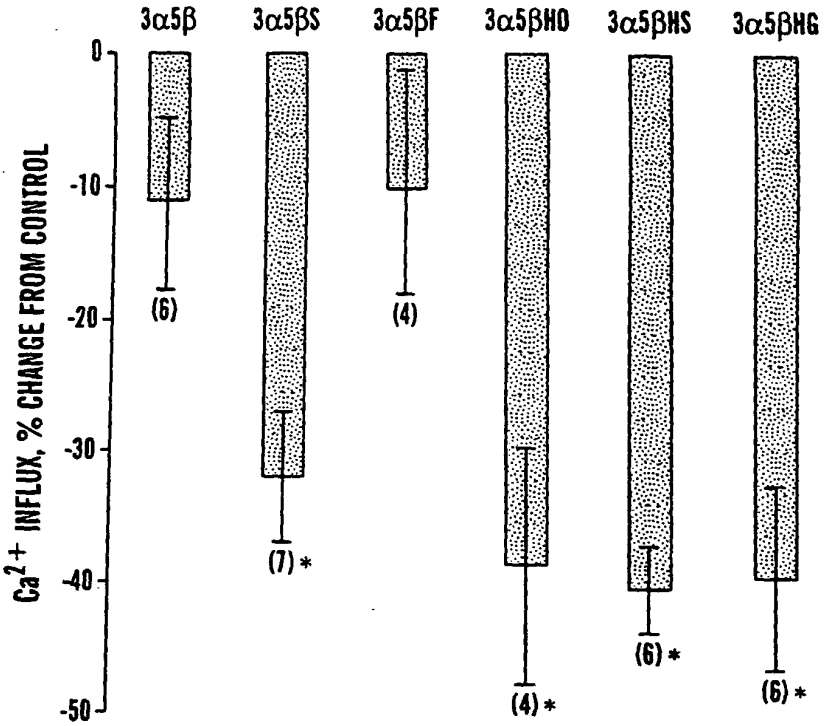
3α5β
3α5βS
3α5βF
3α5βHO
3α5βHS
3α5βHG
0
-10
-20
-30
-40
-50
Ca^{2+} INFLUX, % CHANGE FROM CONTROL
(6)
(7)*
(4)
(4)*
(6)*
(6)*

FIG. 7C

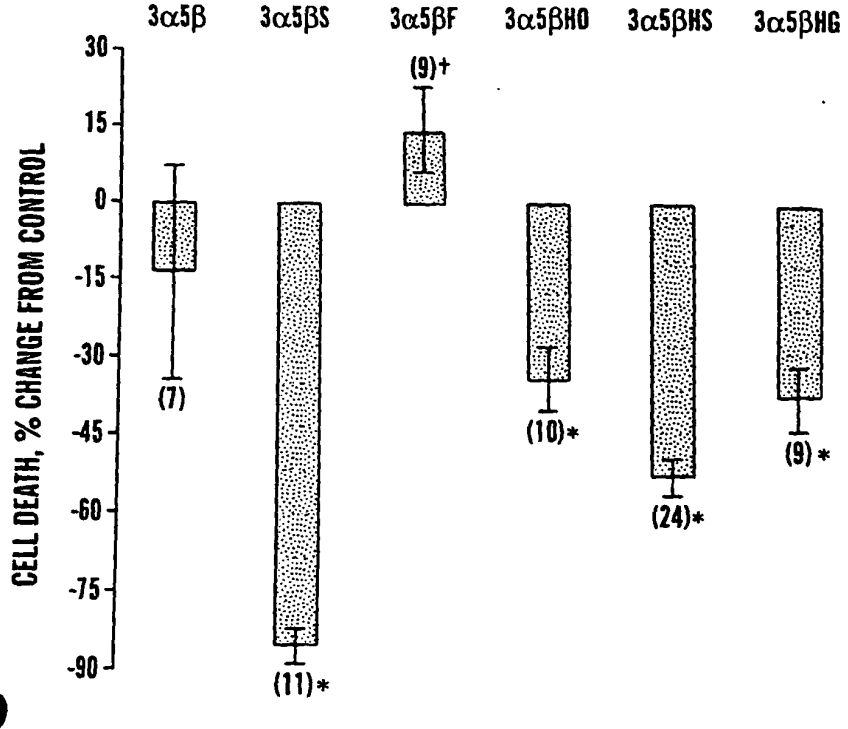
3α5β
3α5βS
3α5βF
3α5βHO
3α5βHS
3α5βHG
30
15
0
-15
-30
-45
-60
-75
-90
CELL DEATH, % CHANGE FROM CONTROL
(7)
(11)*
(9)†
(10)*
(24)*
(9)*

FIG. 7D

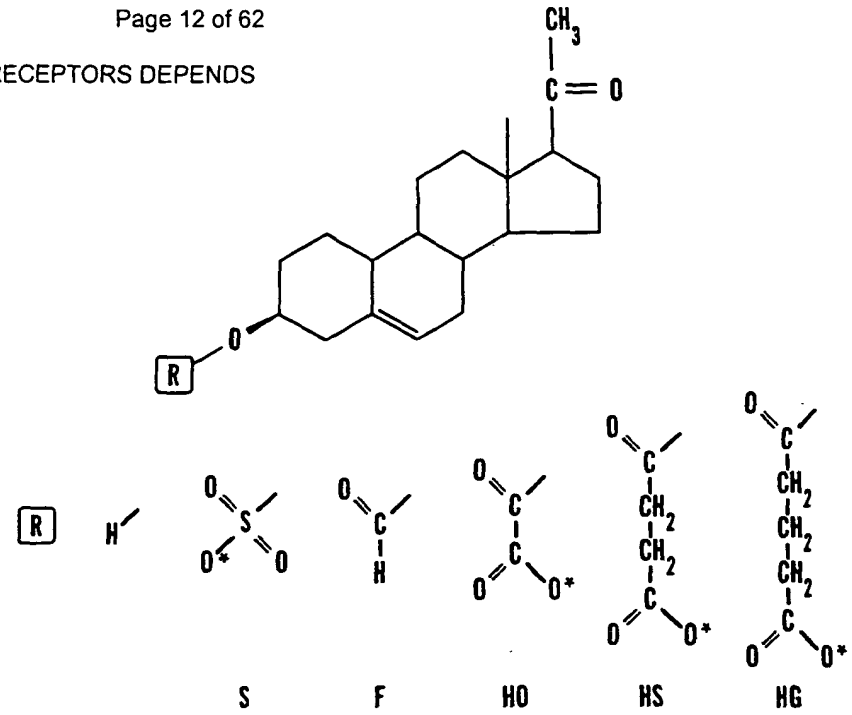
CH3
C = O
O
R
R
H
O
S
O*
O
O
C
H
O
C
C
O
O*
O
C
CH2
CH2
C
O
O*
O
C
CH2
CH2
CH2
C
O
O*
S
F
HO
HS
HG

FIG. 8A

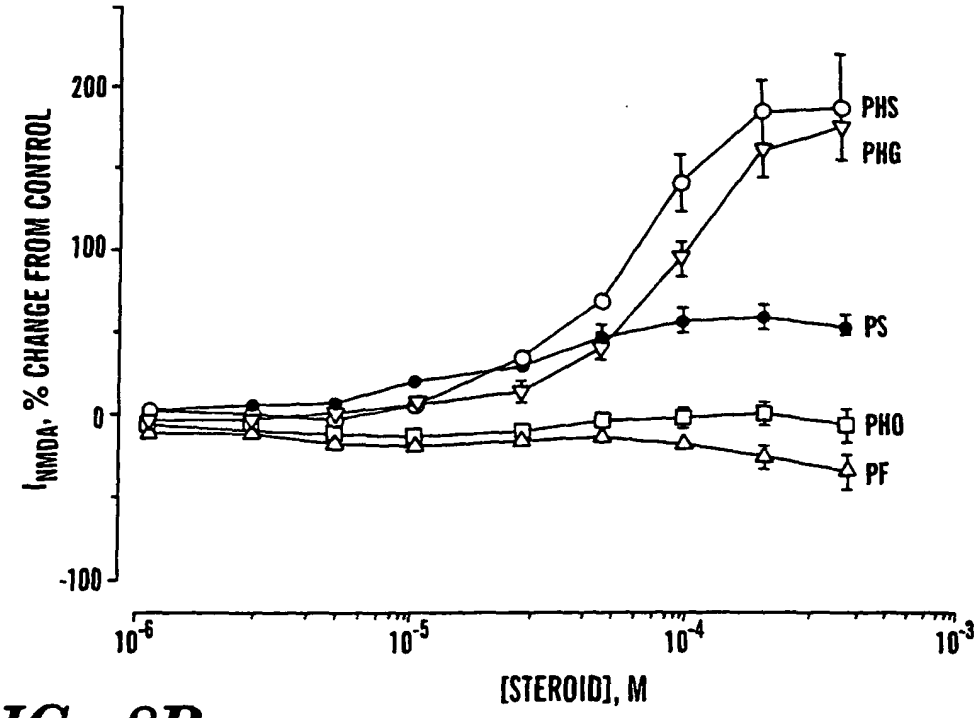
200
100
0
-100
I_{NMDA}, % CHANGE FROM CONTROL
PHS
PHG
PS
PHO
PF
10^{-6}
10^{-5}
10^{-4}
10^{-3}
[STEROID], M

FIG. 8B

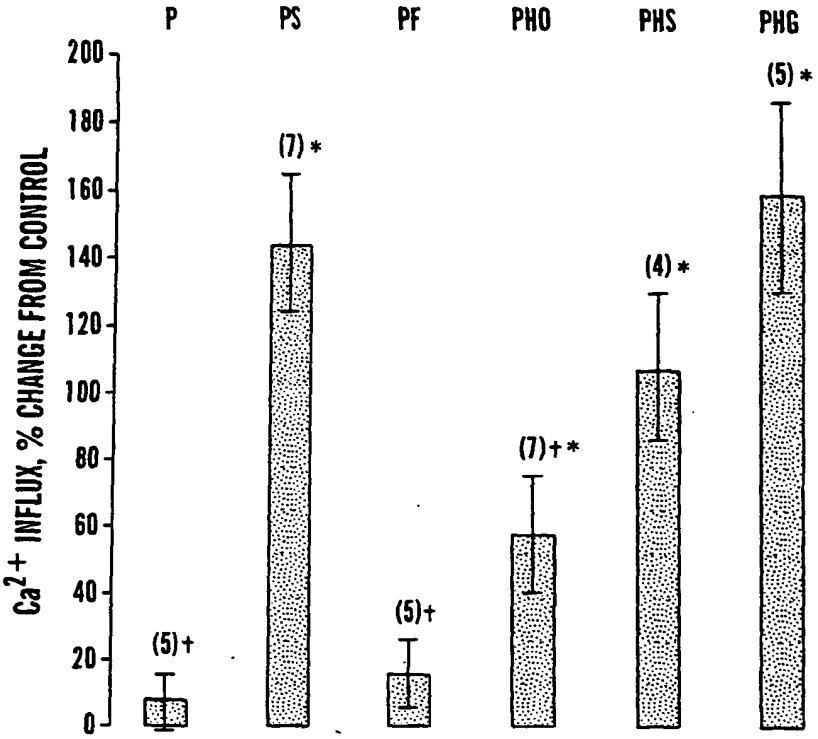
P
PS
PF
PHO
PHS
PHG
200
180
160
140
120
100
80
60
40
20
0
Ca^{2+} INFLUX, % CHANGE FROM CONTROL
(5)+
(7)*
(5)+
(7)+*
(4)*
(5)*

FIG. 8C

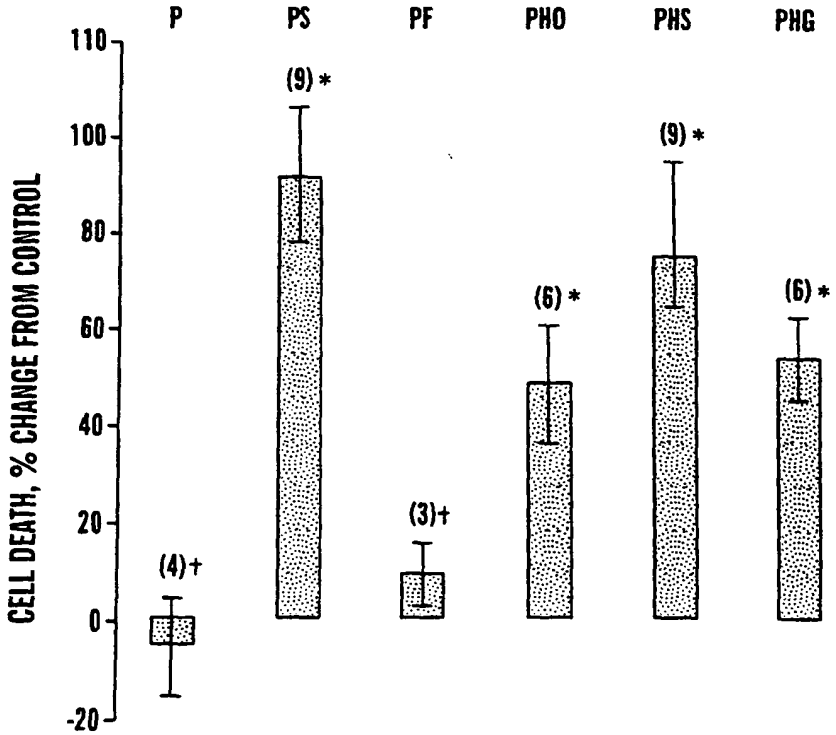
P
PS
PF
PHO
PHS
PHG
110
100
80
60
40
20
0
-20
CELL DEATH, % CHANGE FROM CONTROL
(4)+
(9)*
(3)+
(6)*
(9)*
(6)*

FIG. 8D

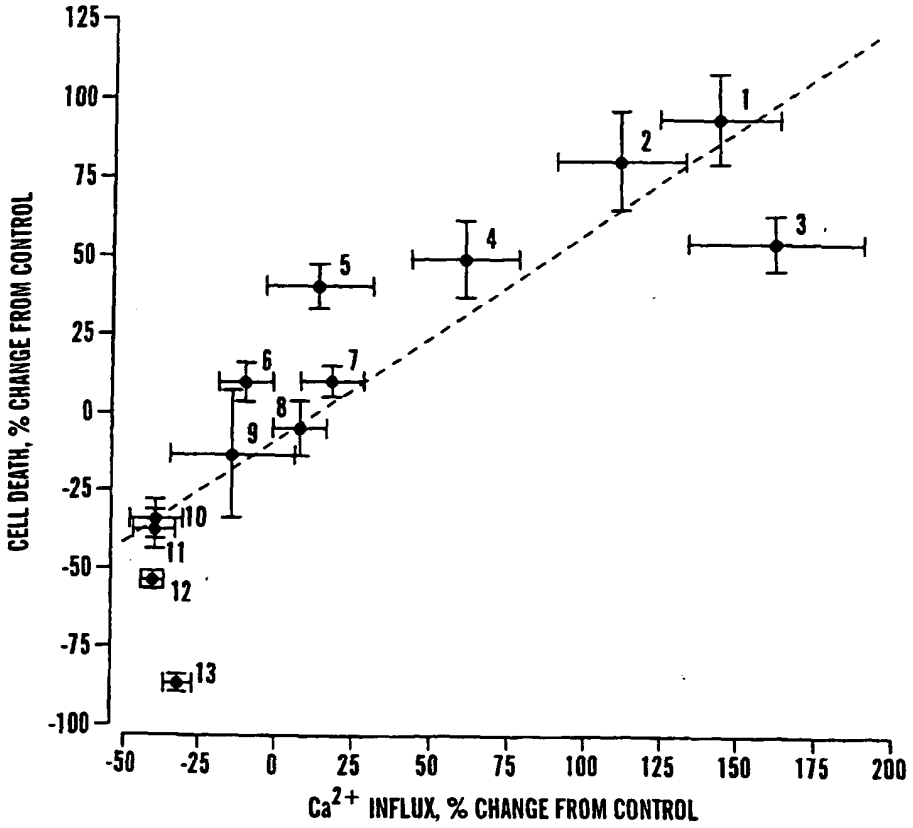
125
100
75
50
25
0
-25
-50
-75
-100
CELL DEATH, % CHANGE FROM CONTROL
-50
-25
0
25
50
75
100
125
150
175
200
Ca2+ INFLUX, % CHANGE FROM CONTROL
1
2
3
4
5
6
7
8
9
10
11
12
13

FIG. 9

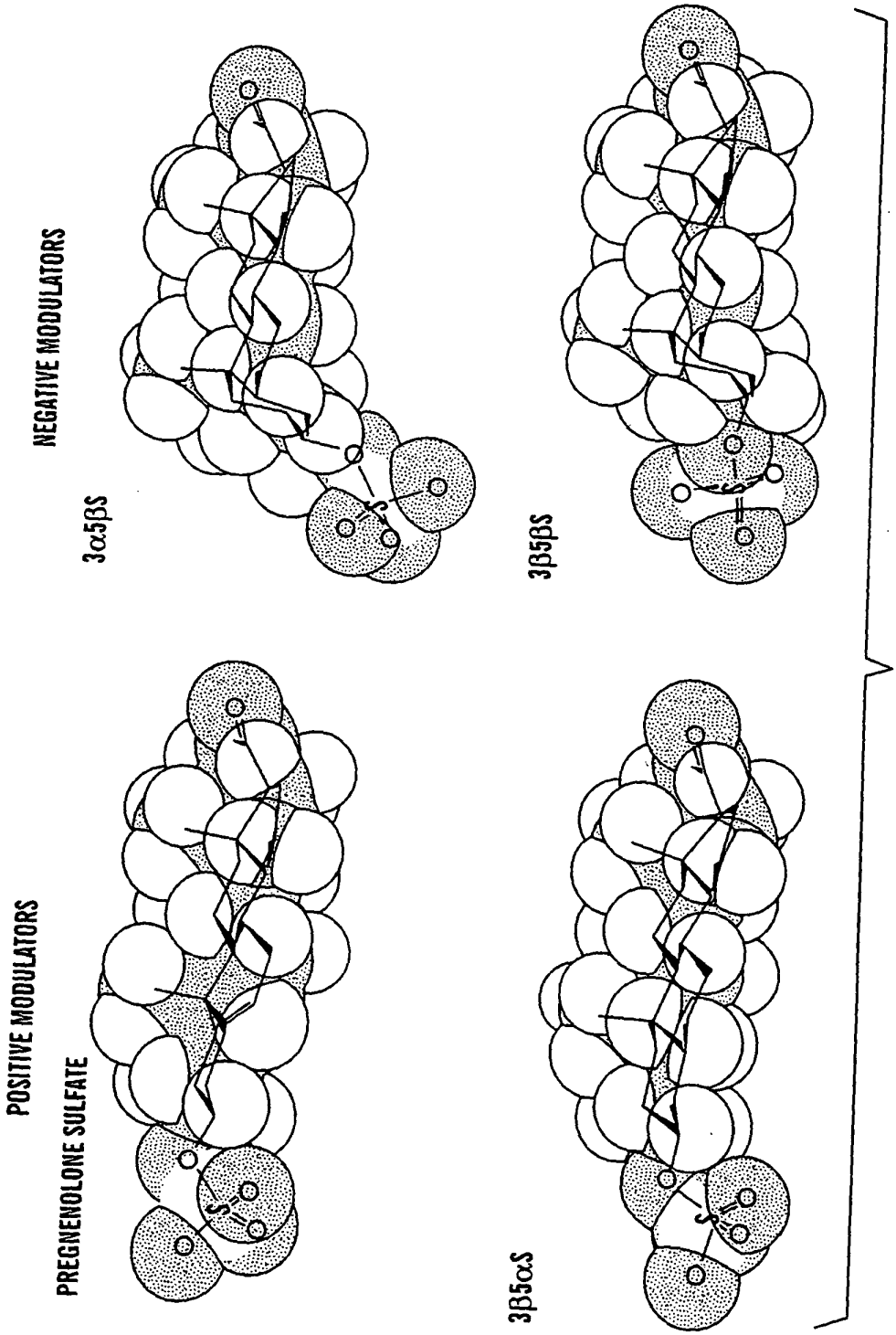
NEGATIVE MODULATORS
3α5βS
3β5βS
POSITIVE MODULATORS
PREGNENOLONE SULFATE
3β5αS

FIG. 10

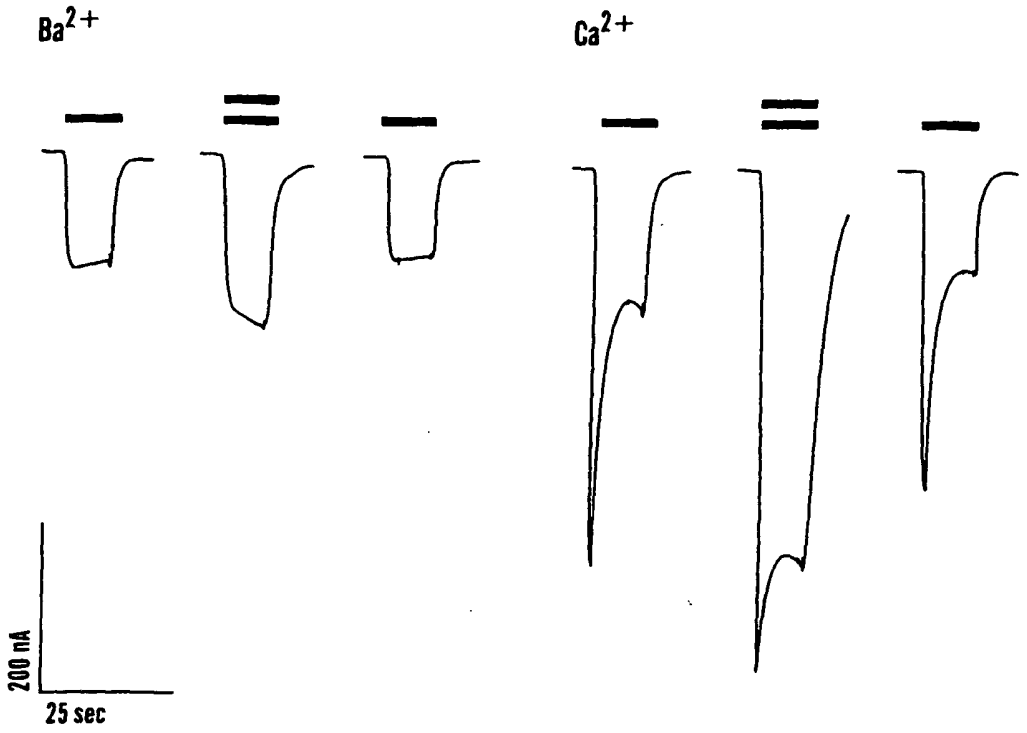

FIG. 11

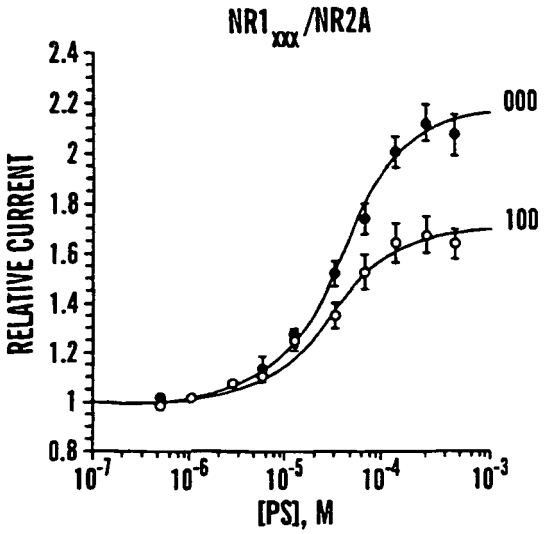

FIG. 12A

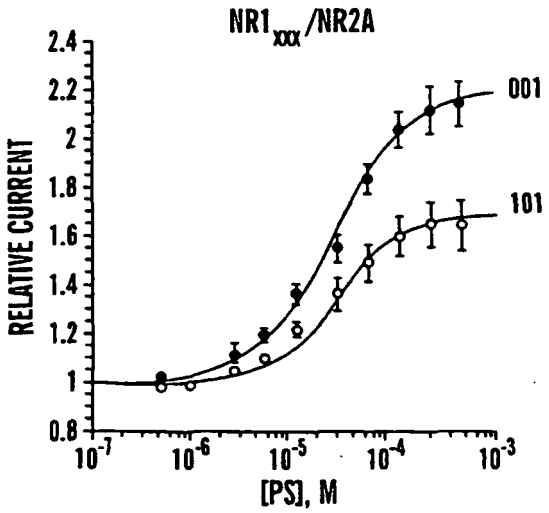

FIG. 12B

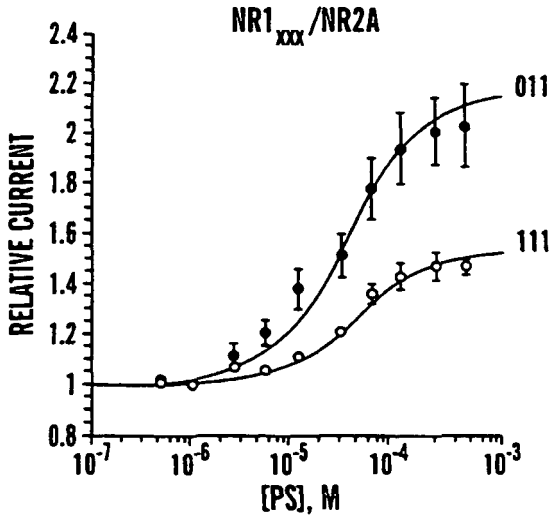

FIG. 12C

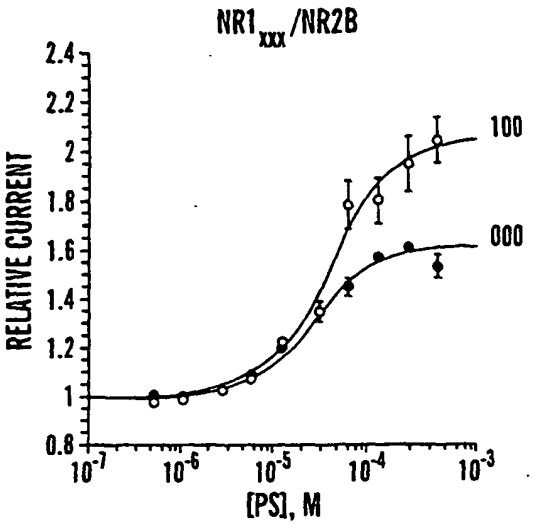

FIG. 13A

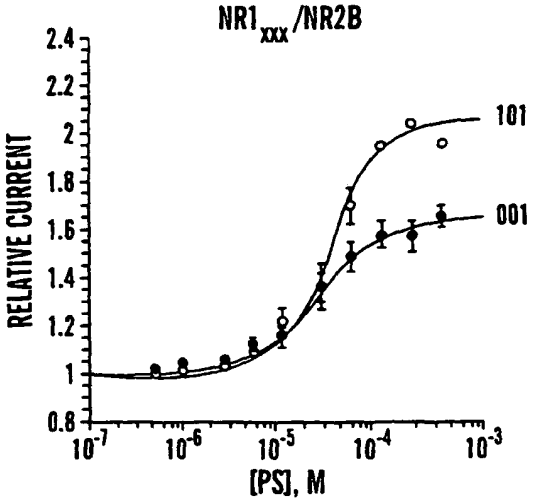

FIG. 13B

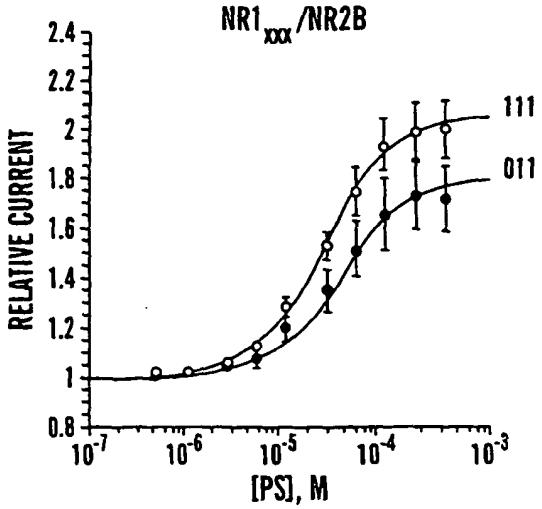

FIG. 13C

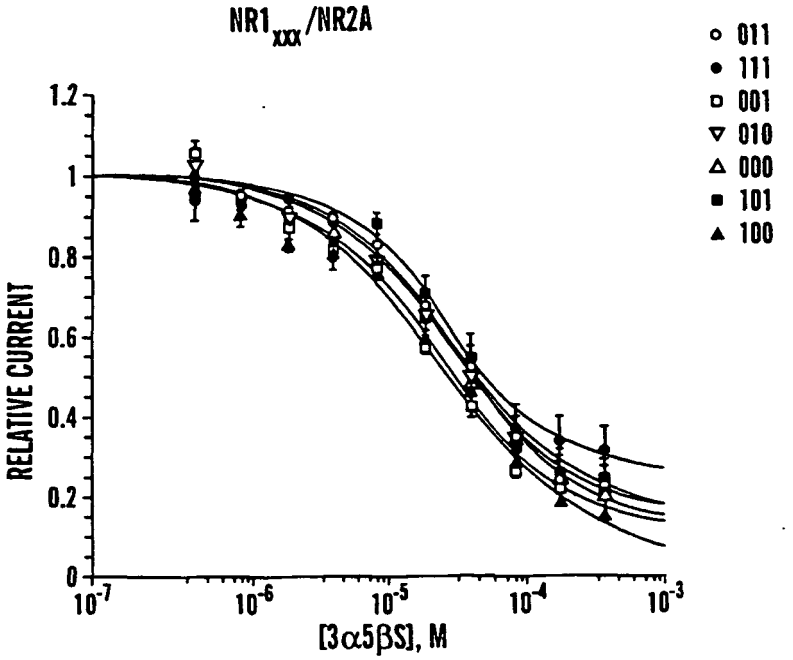

FIG. 14A

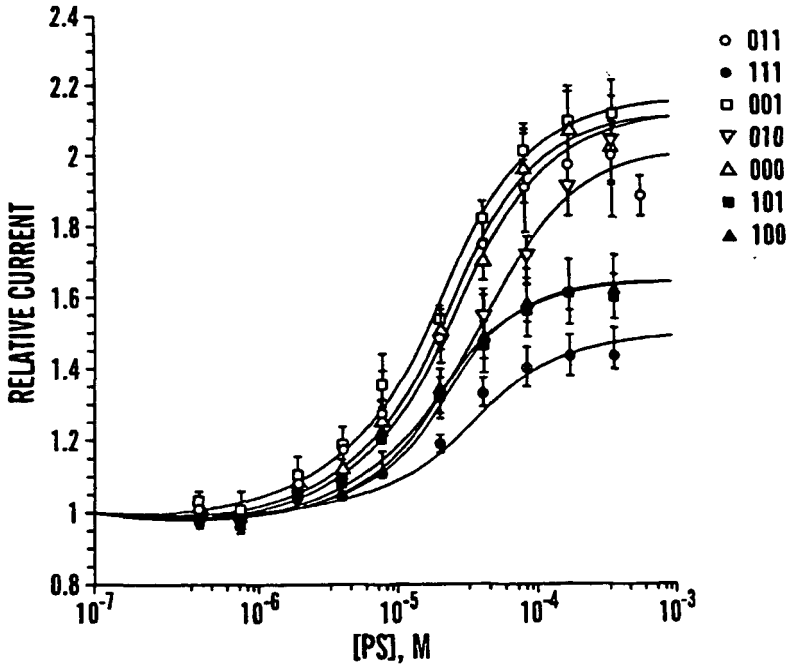

FIG. 14B

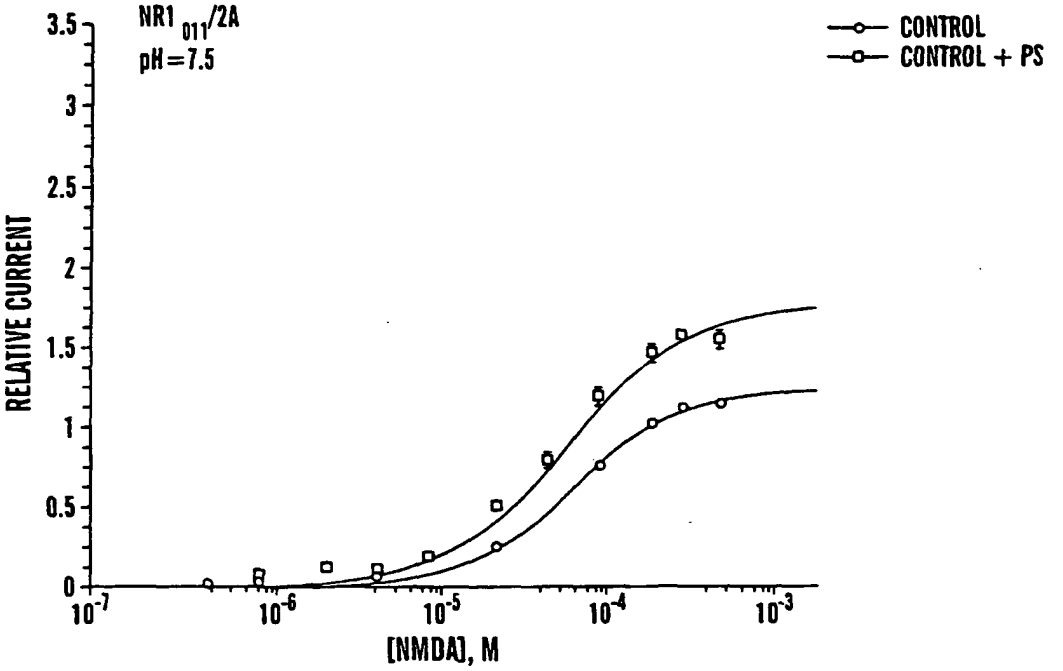

FIG. 15A

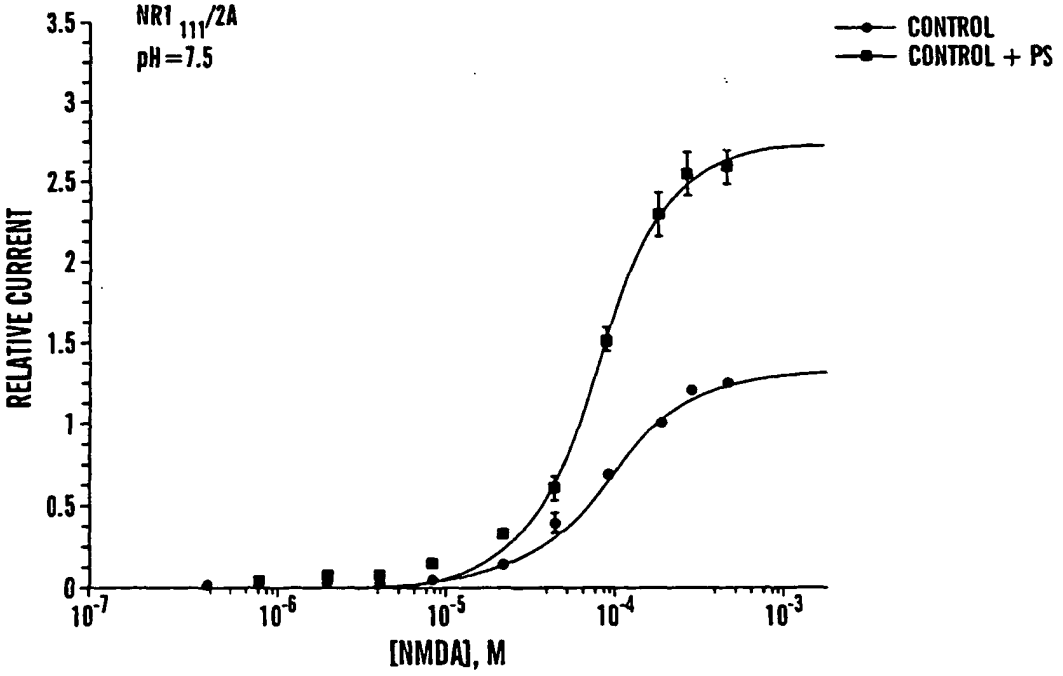

FIG. 15B

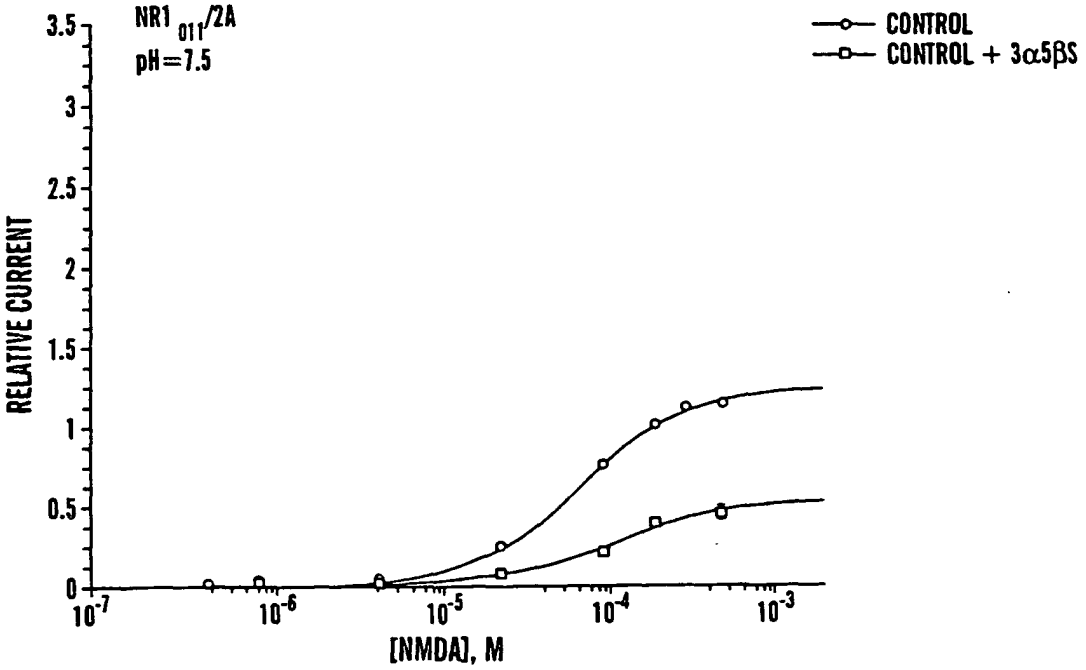

FIG. 16A

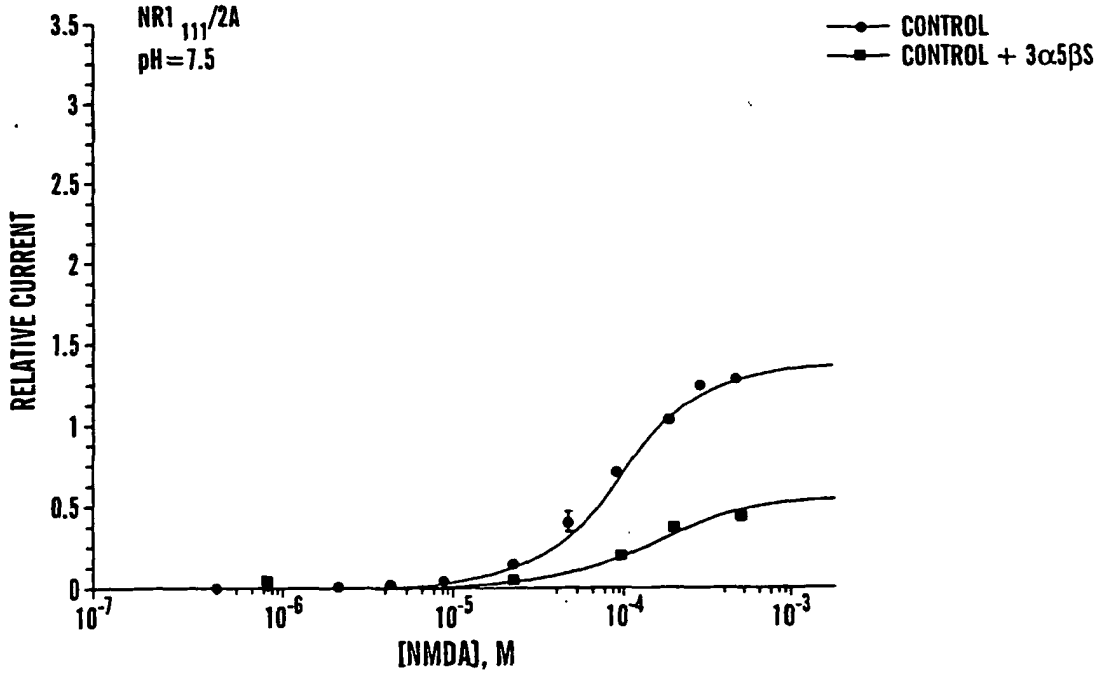

FIG. 16B

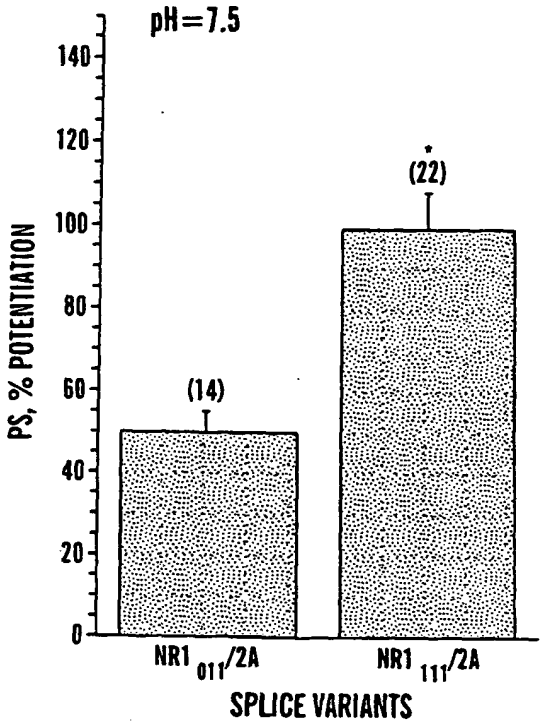

FIG. 17A

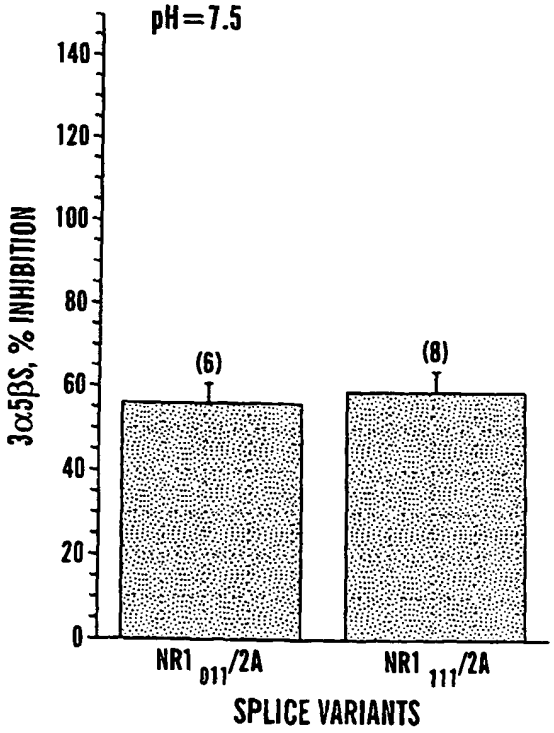

FIG. 17B

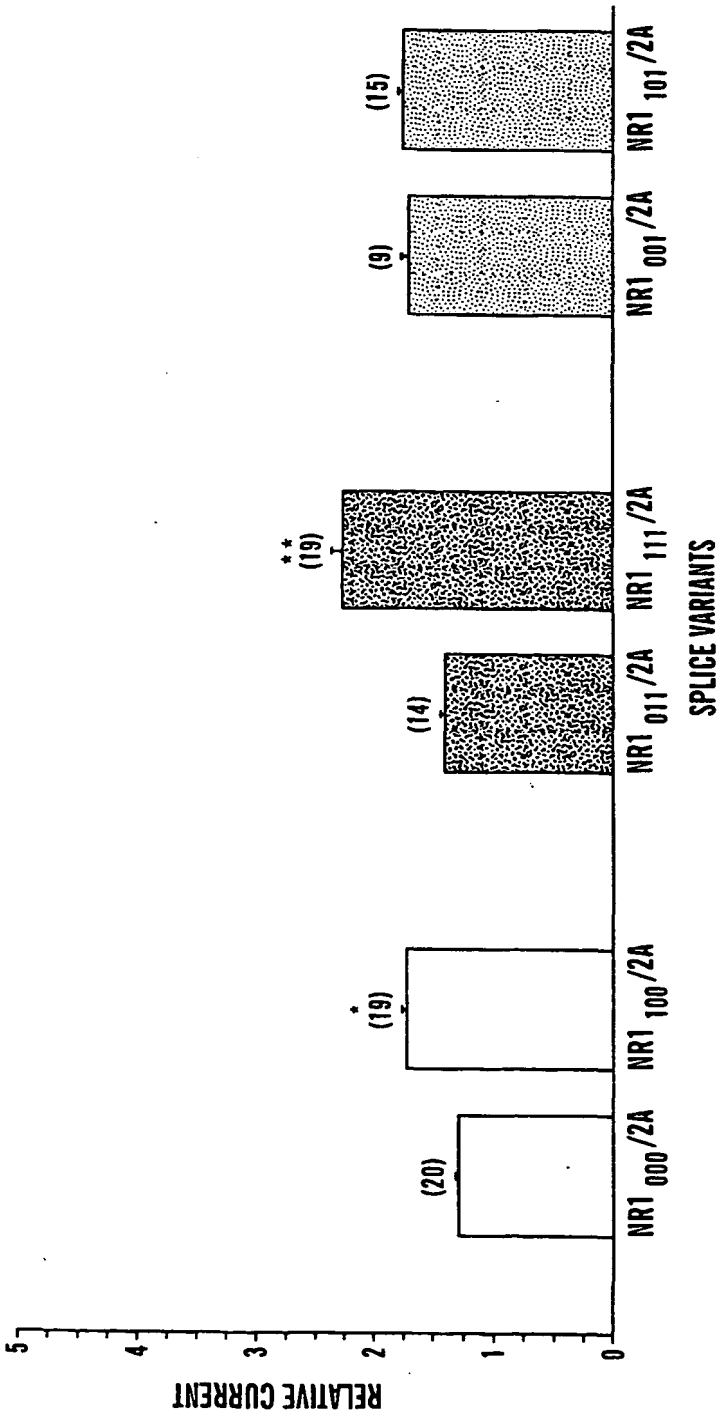
RELATIVE CURRENT
0
1
2
3
4
5
(20)
(19)
(14)
(19)
(9)
(15)
NR1 000/2A
NR1 100/2A
NR1 011/2A
NR1 111/2A
NR1 001/2A
NR1 101/2A
SPLICE VARIANTS

FIG. 18

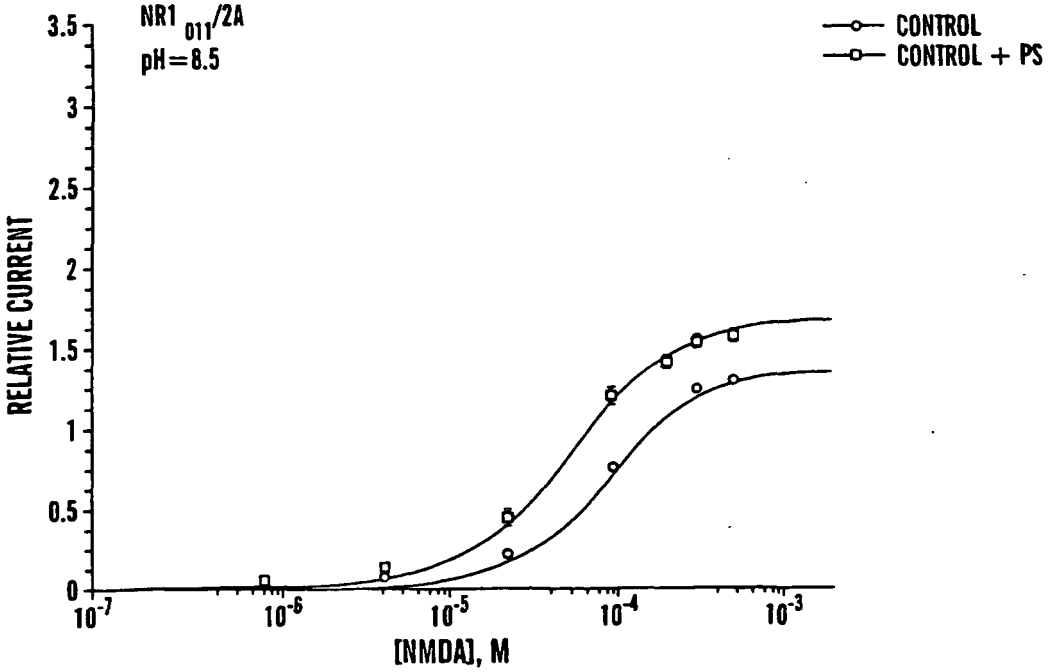

FIG. 19A

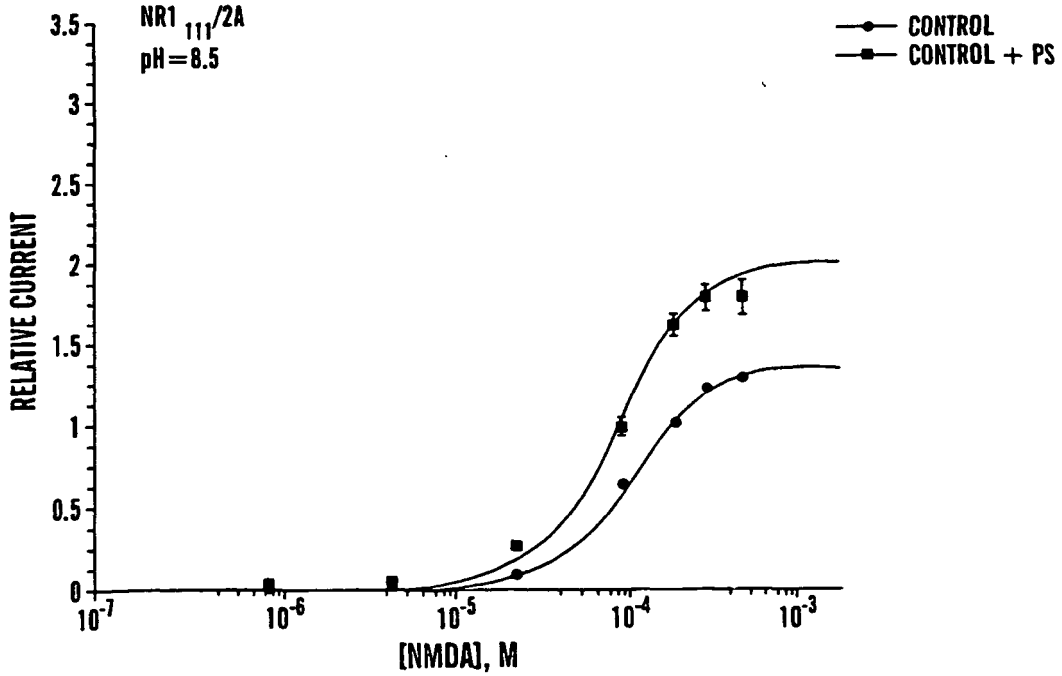

FIG. 19B

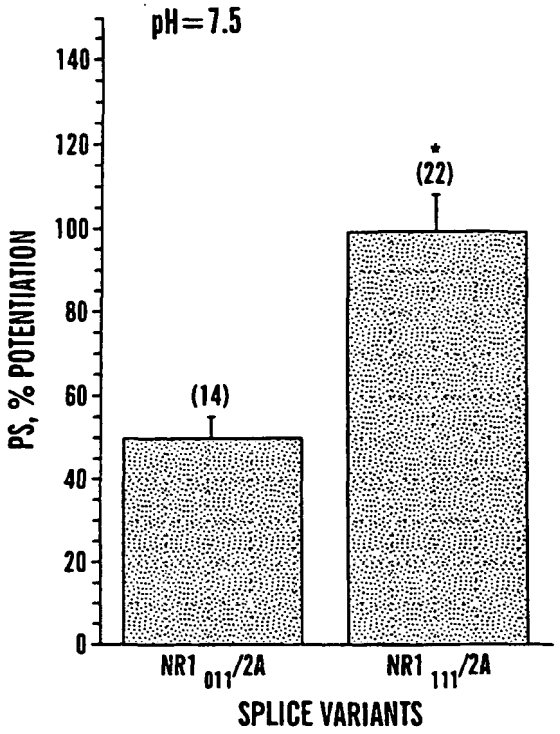

FIG. 20A

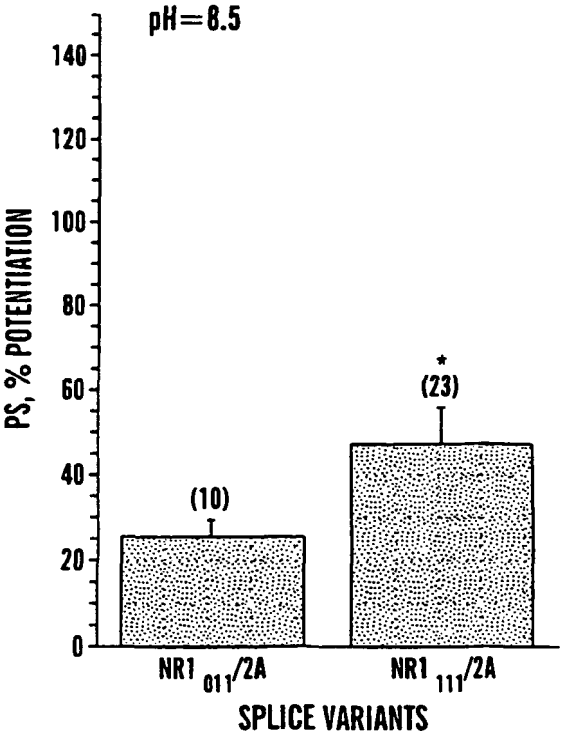

FIG. 20B

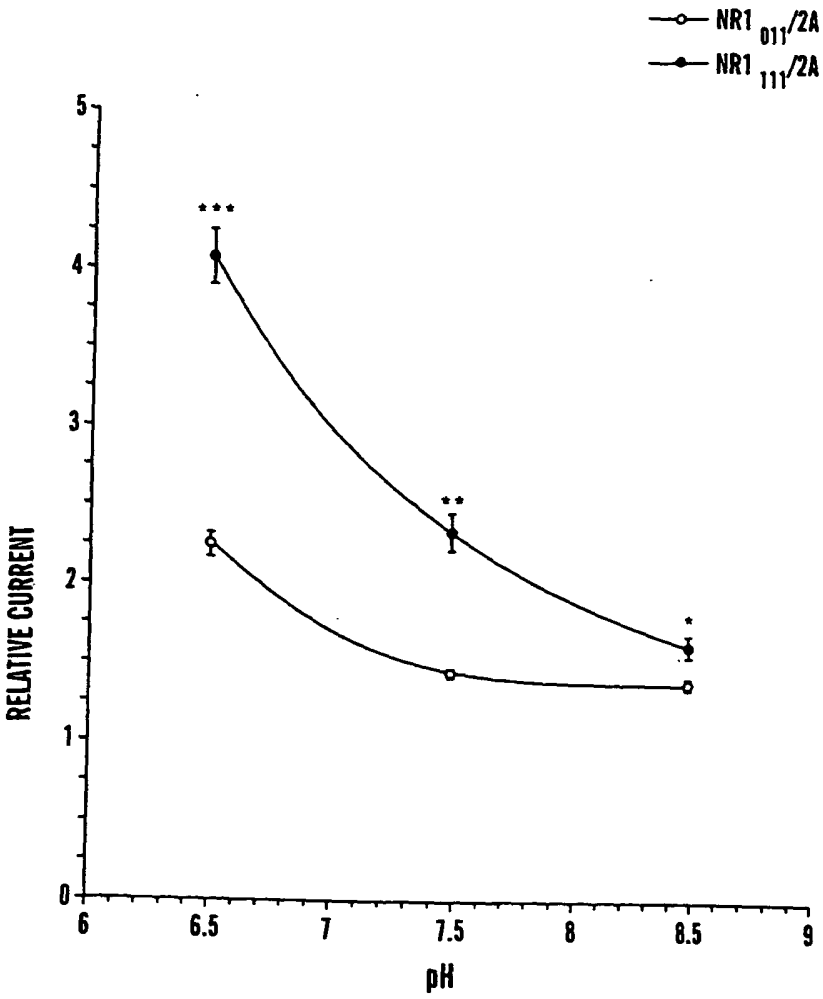

FIG. 21

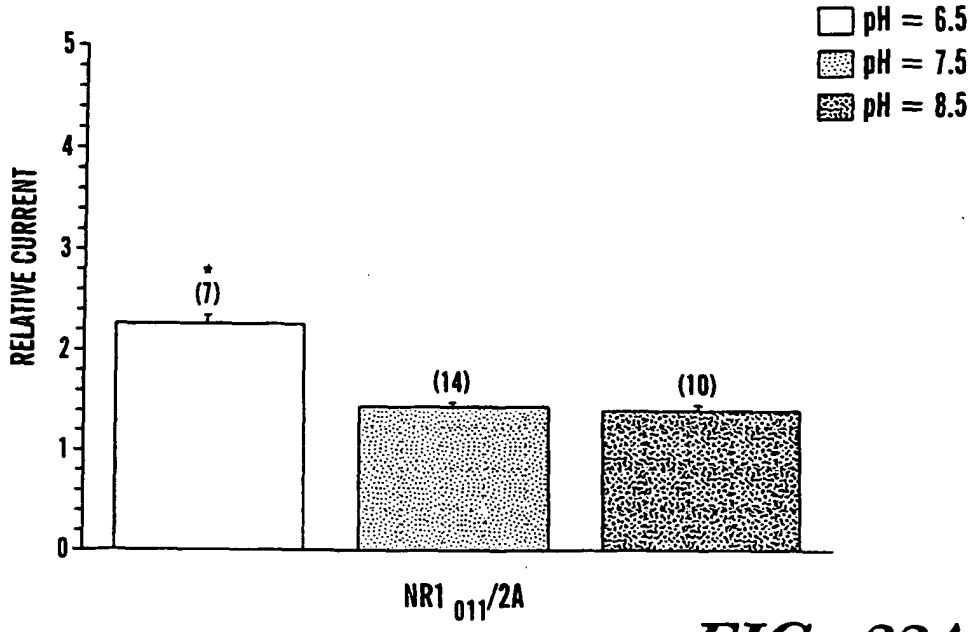

FIG. 22A

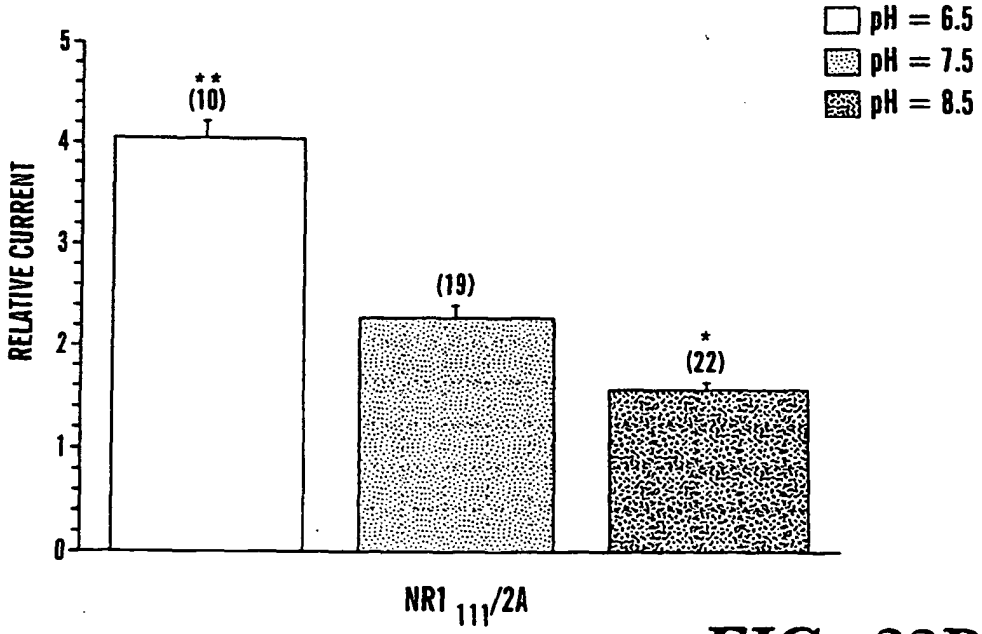

FIG. 22B

```
RXR-α     ILE.AELAVEPKTETYVEANMGL.NPSSPNDPVTNIC.QAADKQLFTL
  RAR     LCQLGKYTTNSSADHRVQLDLGLWDKFS..ELATK.C..II.K....I
   PR     IN.LLM.SIEPDV.IYAGHD.N.TKPDTSSSLLTSL.NQLGERQLLSV
  GCR     VS.LLE.VIEPEV.LYAGYD.S.SVPDSTWRIMTTL.NMLGGRQVIAA
   ER      SALLD.A.EPPI.LYSEYD.P.TRPFSEASMMGLLTN.LADRELVHM
NR1011    IILLVSDDHEGRAA.QKRLETLLEERESKAEKVLQF.DP.GTKNVTAL  207
                                  Δ     Δ         Δ

RXR-α     V.EWAKRIPH.FSELPL..DDQVILLRAGWNELLIA..SFSHR.SIA
  RAR     V.EFAKRLPG.FTGLSI..ADQITLLKAACLDILML..RICTR.YTP
   PR     V.KWSKSLPG.FRNLHI..DDQITLIQYSWMSLMV.FGLGWR.SYK
  GCR     V.KWAKAIPG.FRNLHL..DDQMTLLQYSWMFLMA.FALGWR.SYR
   ER     I.NWAKRVPG.FVDLTL..HDQVHLLECAWLEILMI..GLVWR.SME
NR1011    LME.ARELEARVIILSASEDDAATVYRAAAM.LNMTGSGYVWLVGER  252
                                  Δ                   Δ

RXR-α     VKDG.IL.LATG.LH.VHR.N
  RAR     EQDT.MT.FSDG.LT.LNR
   PR     HVSGQMLYFAPD.LI.L...N
  GCR     QSSANLLCFAPD.LI.I...N
   ER     H.PGKLL.FAPN.LL.LDR.N
NR1011    EISGNALRYAPDGIIGLQLIN  273
```

FIG. 23

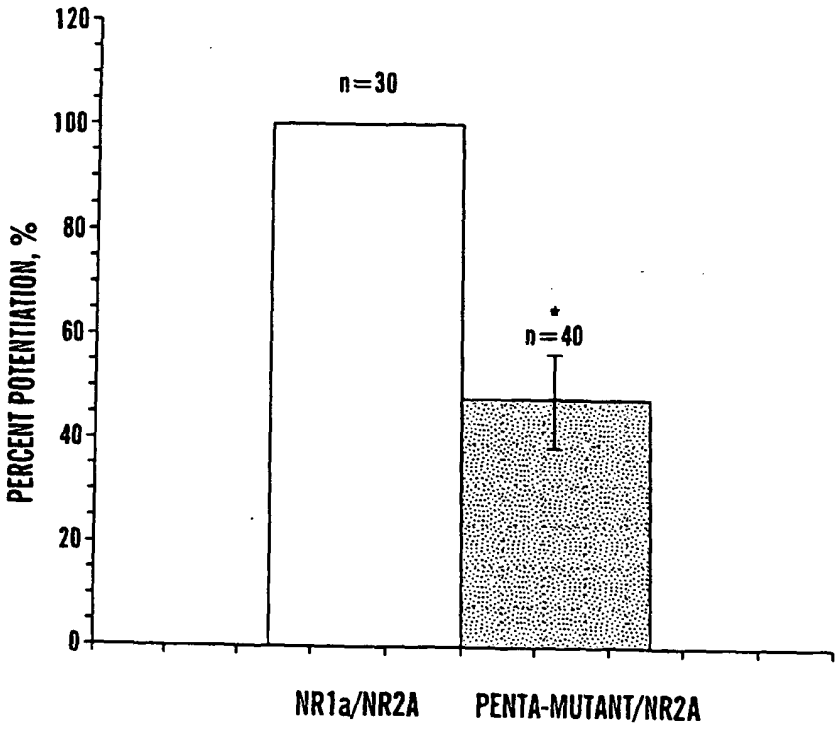
120
100
80
60
40
20
0
PERCENT POTENTIATION, %
n=30
n=40
*
NR1a/NR2A
PENTA-MUTANT/NR2A

FIG. 24

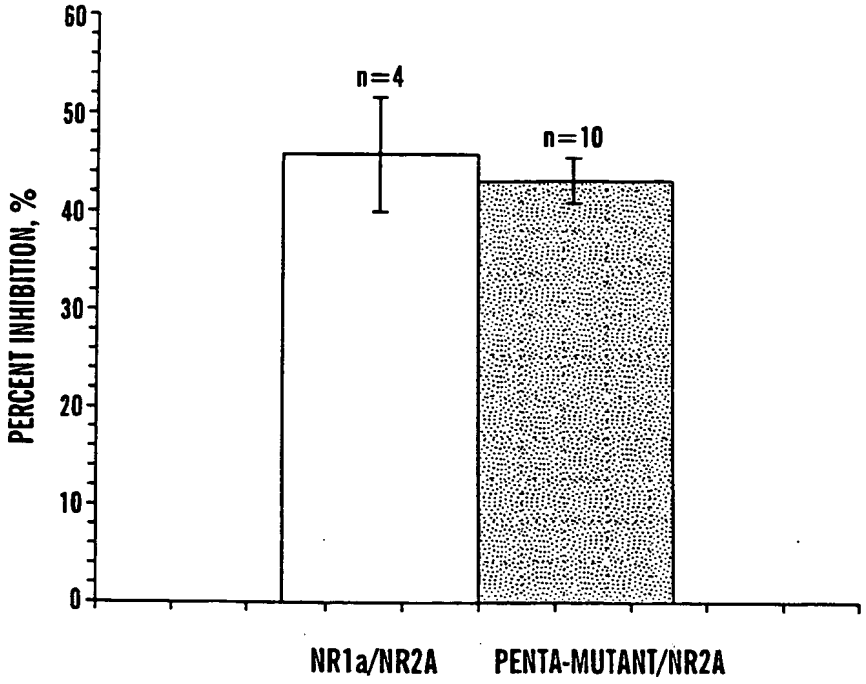
60
50
40
30
20
10
0
PERCENT INHIBITION, %
n=4
n=10
NR1a/NR2A
PENTA-MUTANT/NR2A

FIG. 25

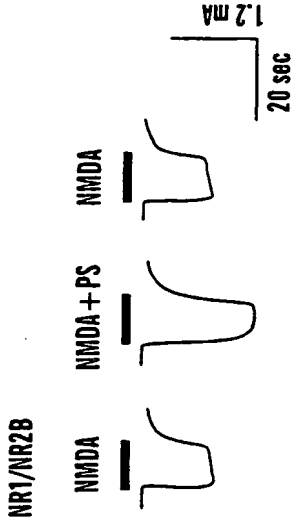

FIG. 26B

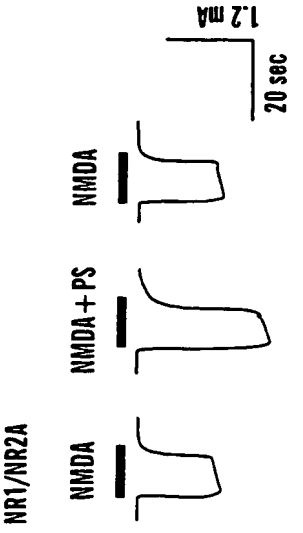

FIG. 26A

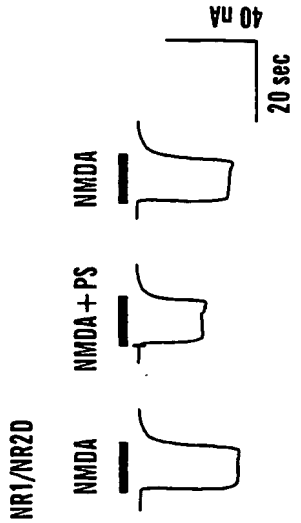

FIG. 26D

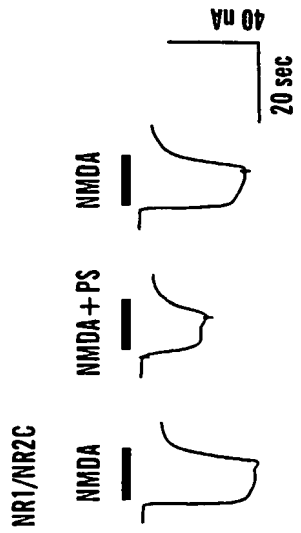

FIG. 26C

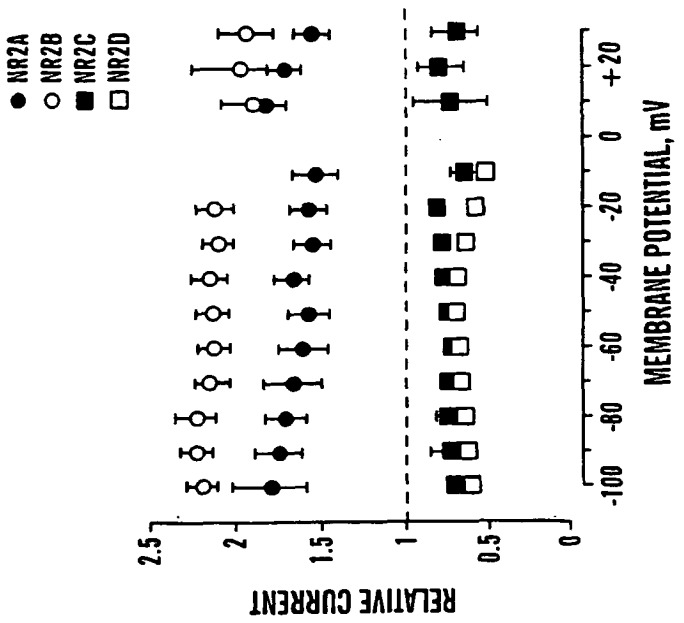

FIG. 26F

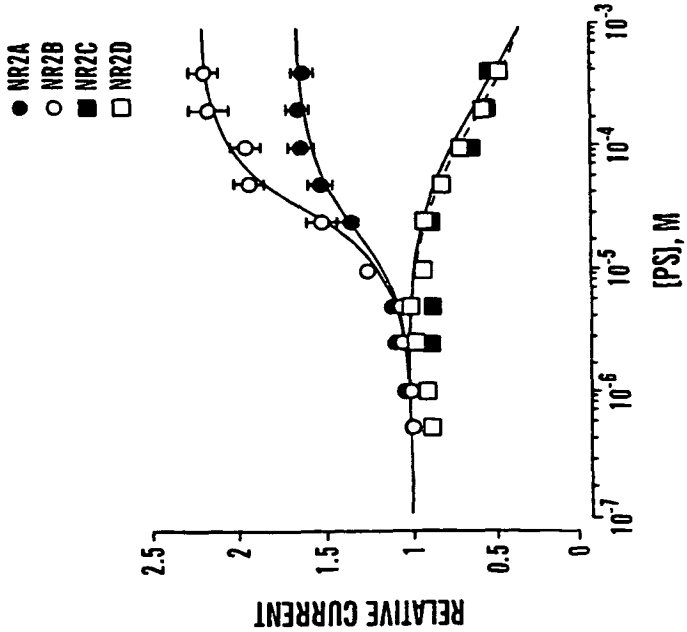

FIG. 26E

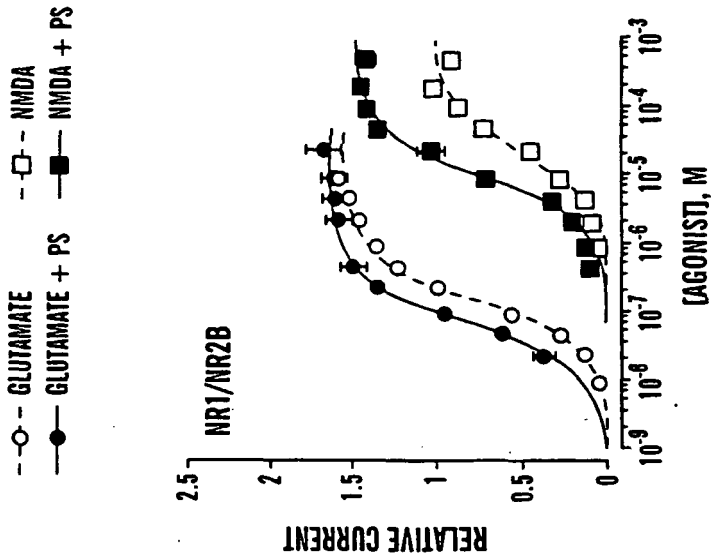

FIG. 27B

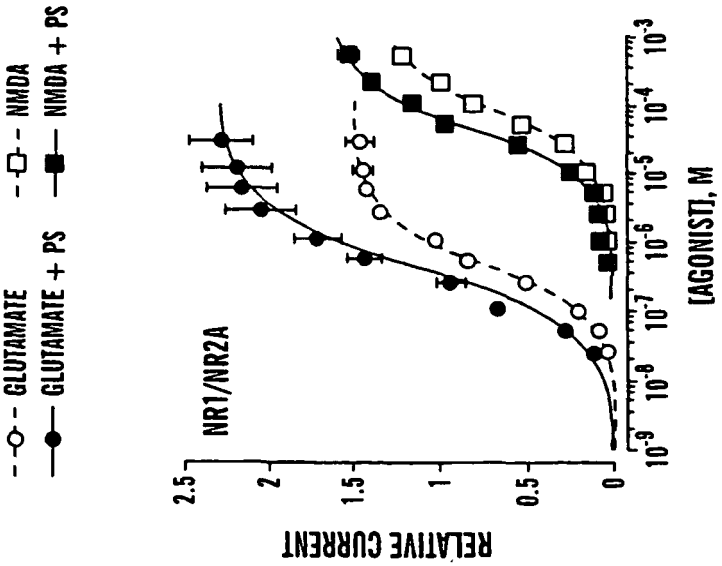

FIG. 27A

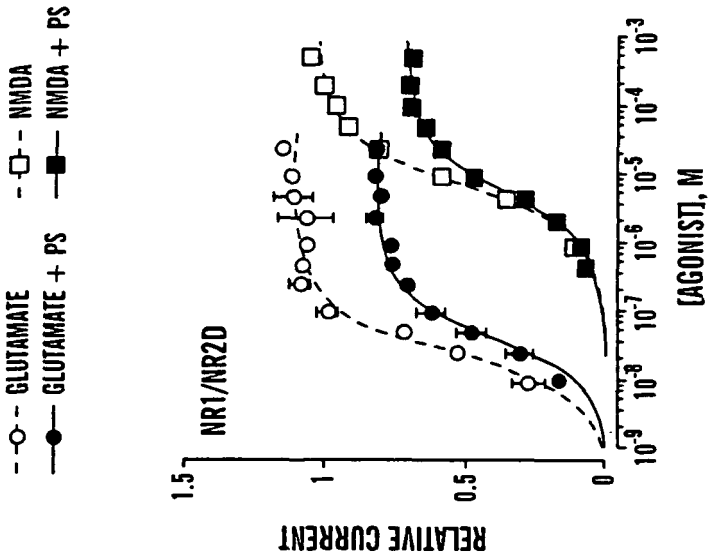

FIG. 27D

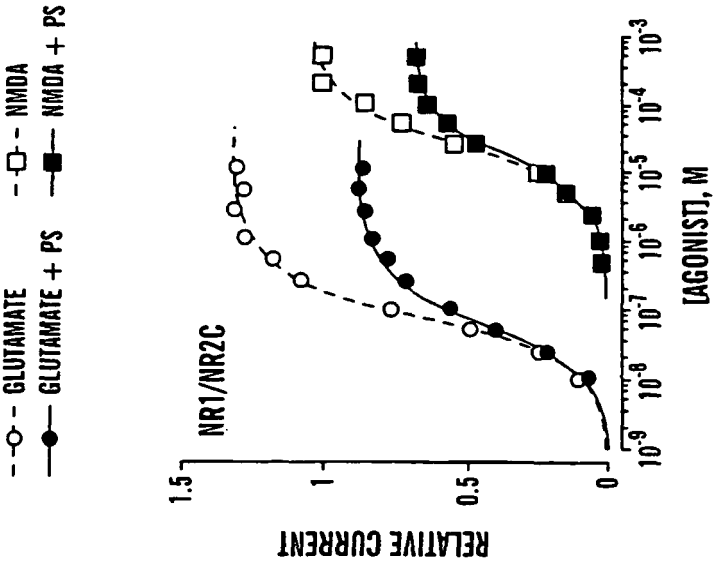

FIG. 27C

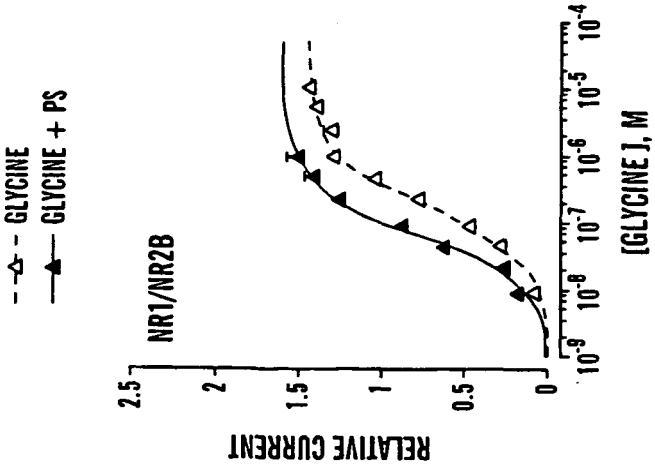

FIG. 28B

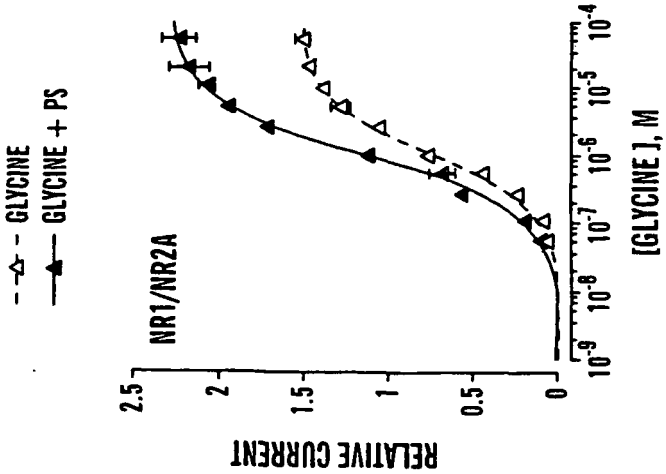

FIG. 28A

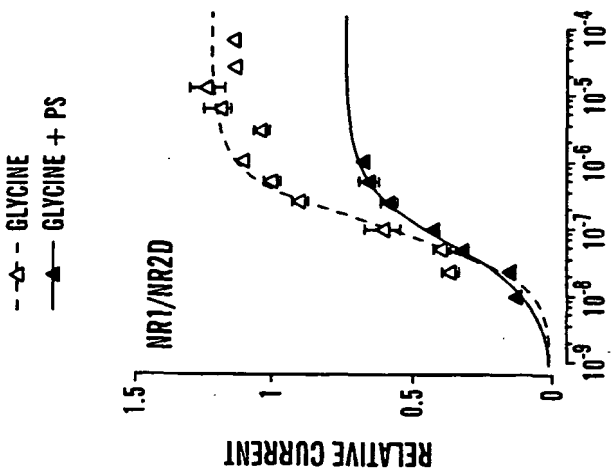

FIG. 28D

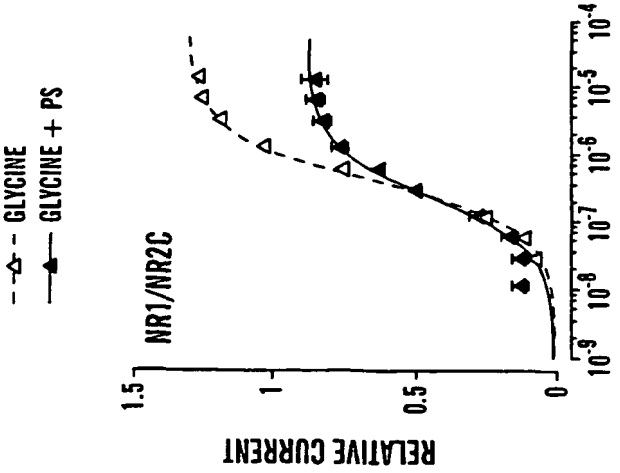

FIG. 28C

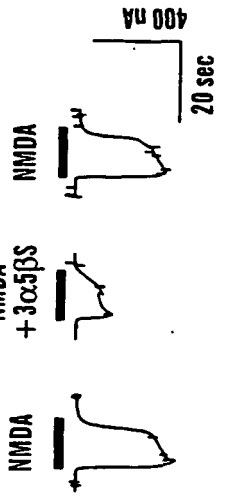

FIG. 29A

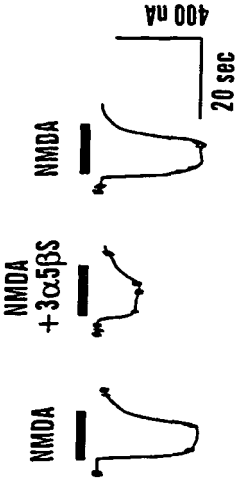

FIG. 29B

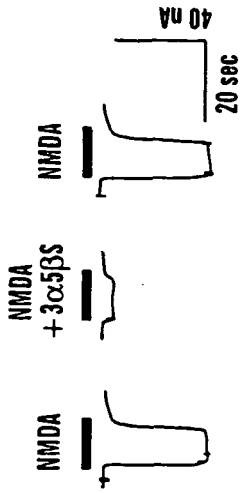

FIG. 29C

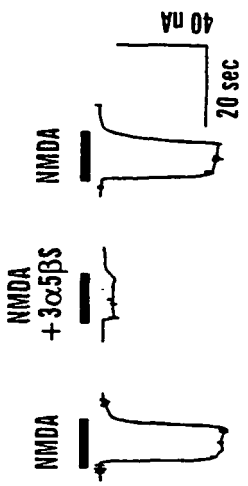

FIG. 29D

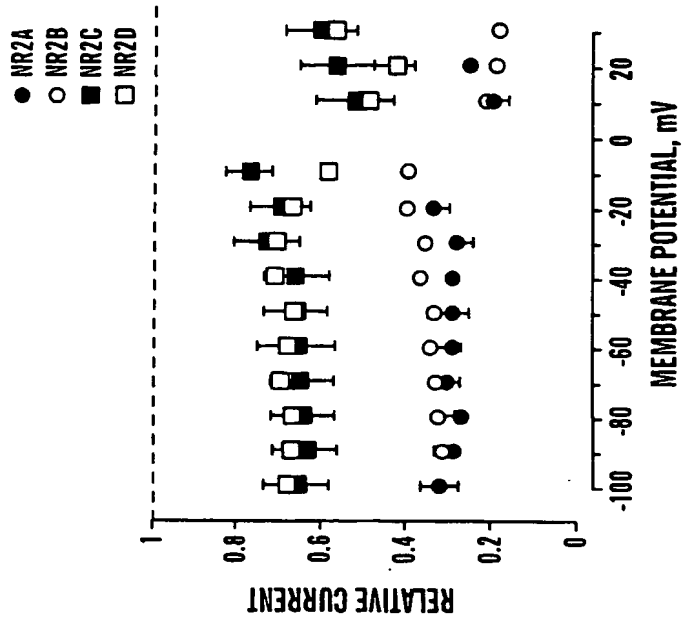

FIG. 29F

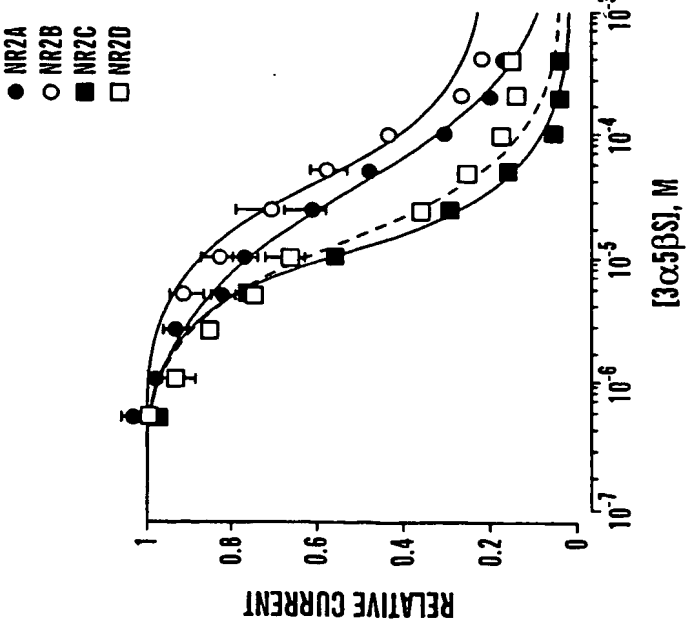

FIG. 29E

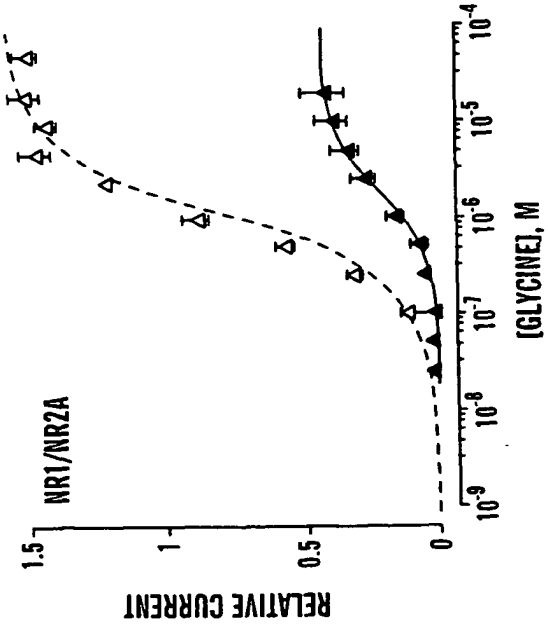

FIG. 29H

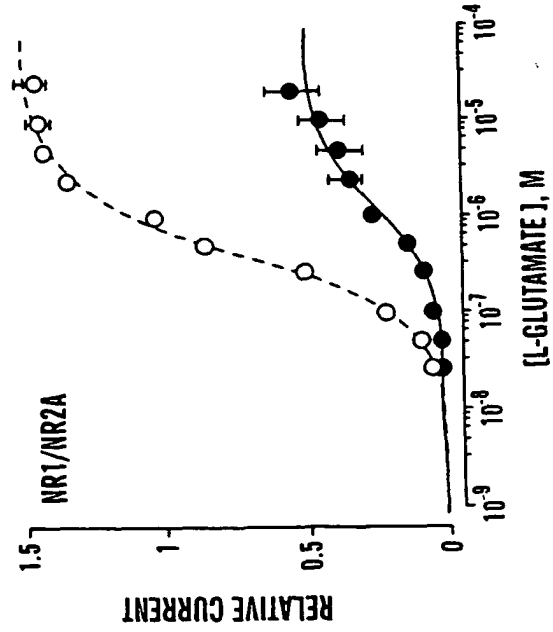

FIG. 29G

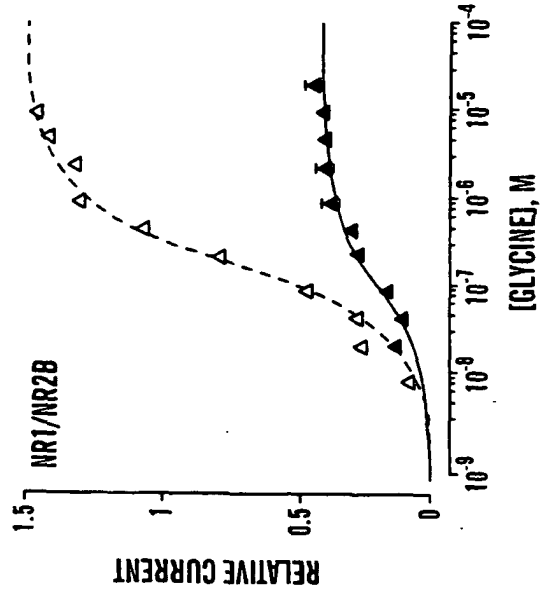

FIG. 29J

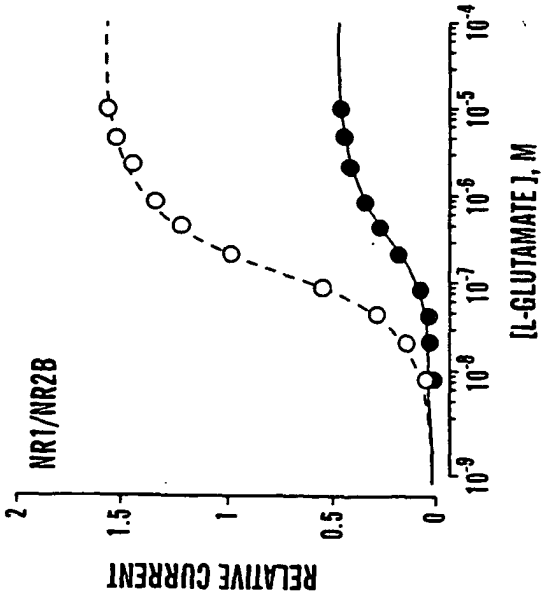

FIG. 29I

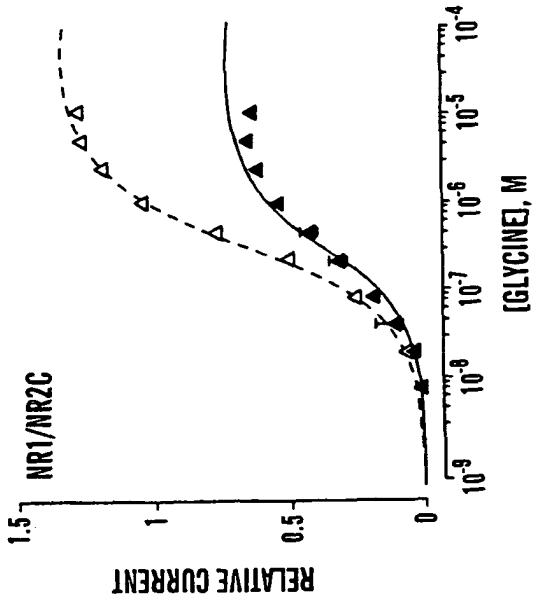

FIG. 29L

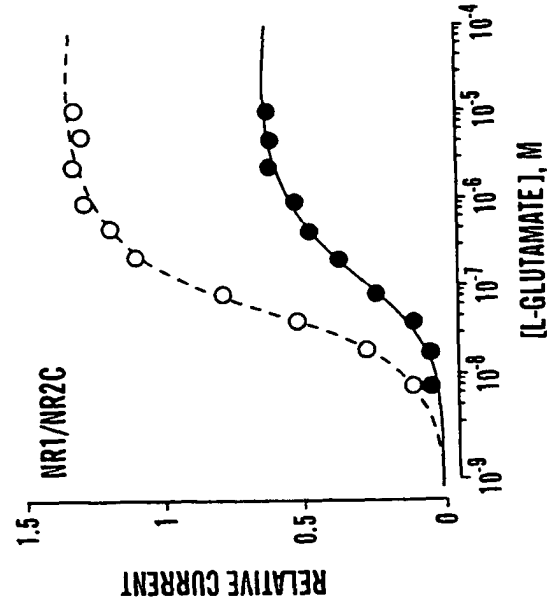

FIG. 29K

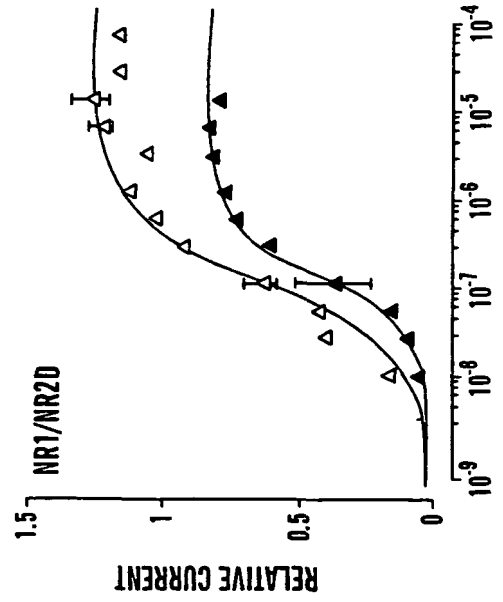

FIG. 29N

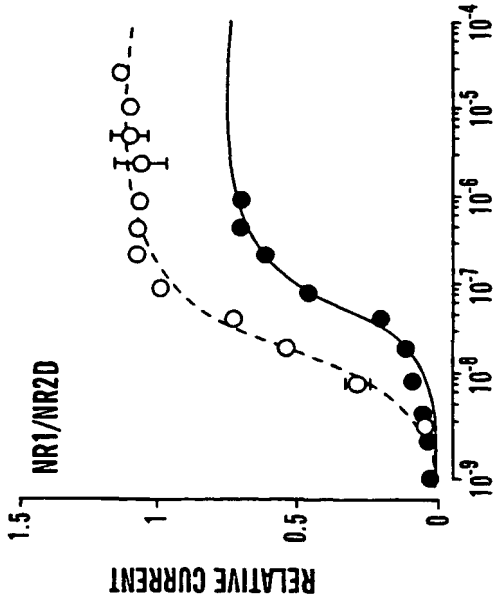

FIG. 29M

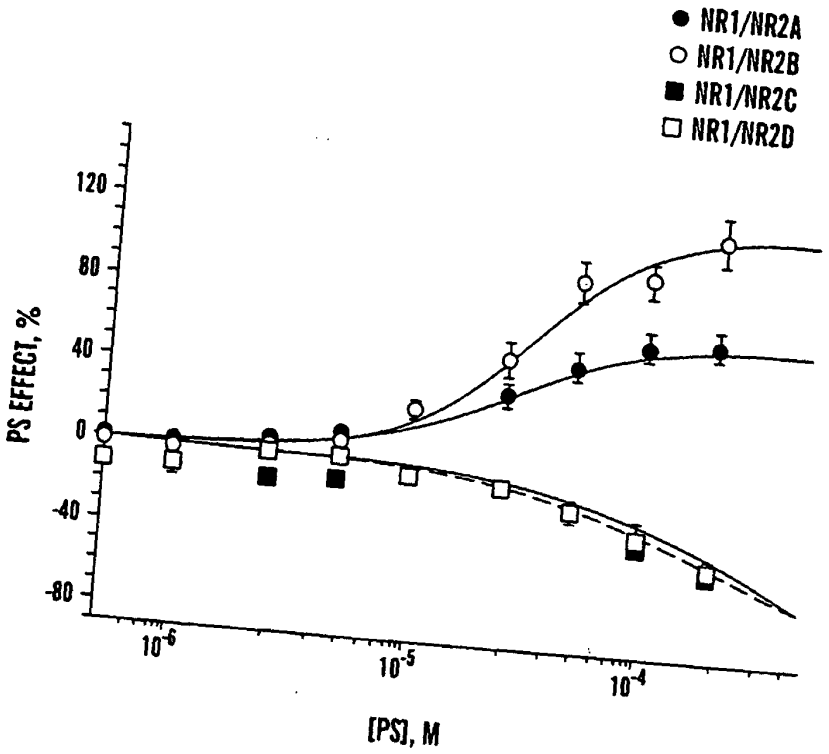
NR1/NR2A
NR1/NR2B
NR1/NR2C
NR1/NR2D
PS EFFECT, %
120
80
40
0
-40
-80
10^-6
10^-5
10^-4
[PS], M

FIG. 30

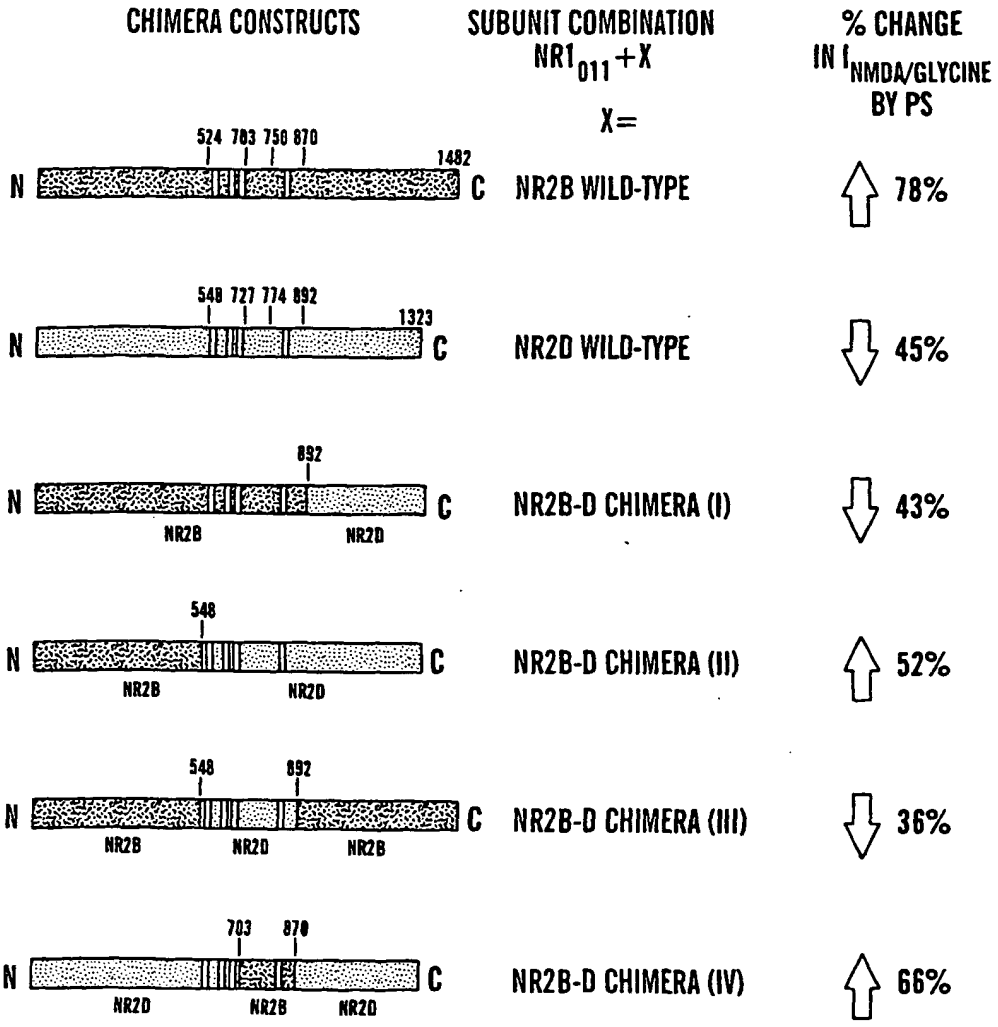
CHIMERA CONSTRUCTS
SUBUNIT COMBINATION
NR1011+X
X=
% CHANGE
IN INMDA/GLYCINE
BY PS
524 703 750 870
1482
N
C
NR2B WILD-TYPE
78%
548 727 774 892
1323
N
C
NR2D WILD-TYPE
45%
892
N
C
NR2B
NR2D
NR2B-D CHIMERA (I)
43%
548
N
C
NR2B
NR2D
NR2B-D CHIMERA (II)
52%
548
892
N
C
NR2B
NR2D
NR2B
NR2B-D CHIMERA (III)
36%
703
870
N
C
NR2D
NR2B
NR2D
NR2B-D CHIMERA (IV)
66%

FIG. 31

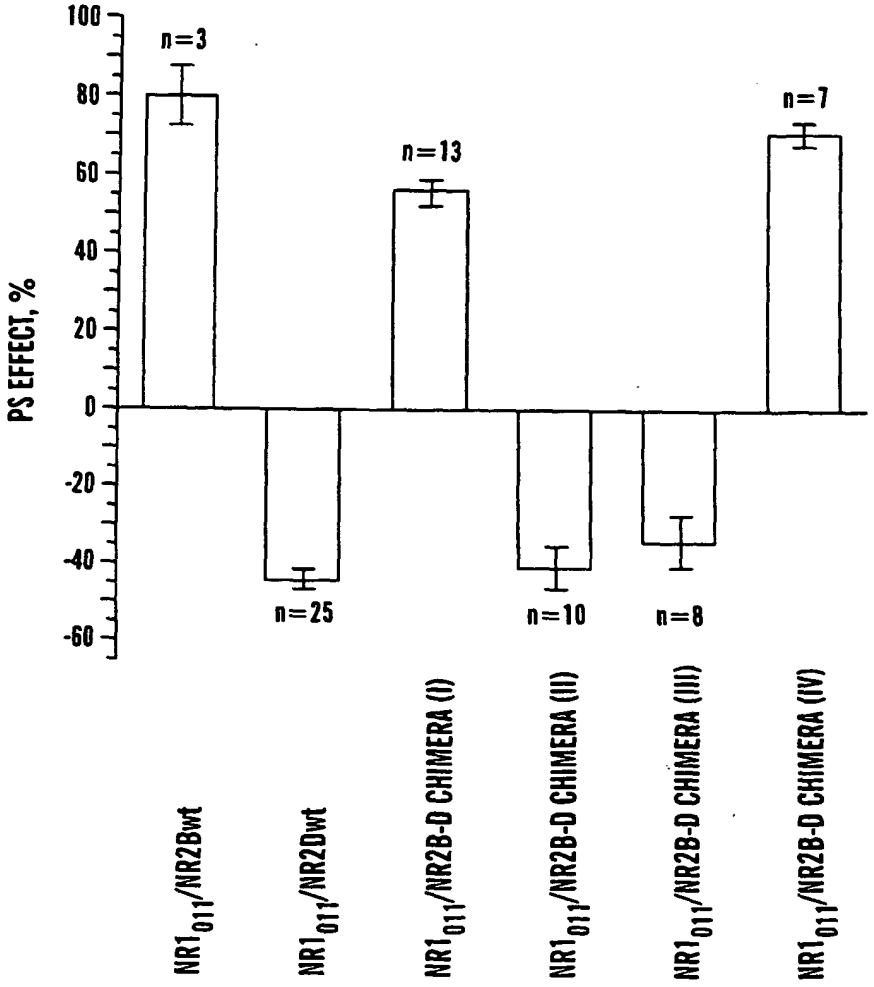
PS EFFECT, %
100
80
60
40
20
0
-20
-40
-60
n=3
n=25
n=13
n=10
n=8
n=7
NR1011/NR2Bwt
NR1011/NR2Dwt
NR1011/NR2B-D CHIMERA (I)
NR1011/NR2B-D CHIMERA (II)
NR1011/NR2B-D CHIMERA (III)
NR1011/NR2B-D CHIMERA (IV)

FIG. 32

FIGURE 33

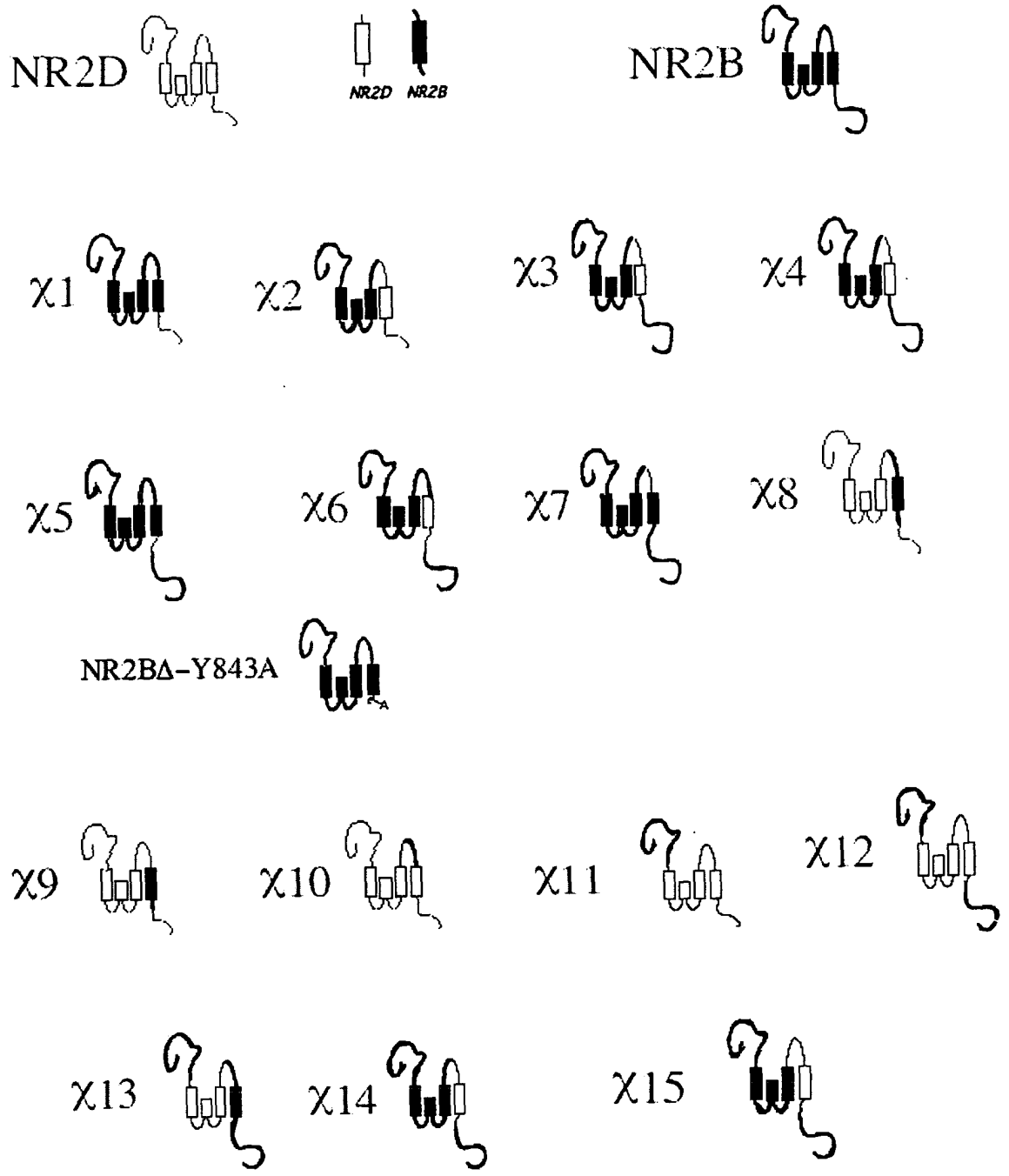
NR2D
NR2D NR2B
NR2B
χ1
χ2
χ3
χ4
χ5
χ6
χ7
χ8
NR2BΔ-Y843A
χ9
χ10
χ11
χ12
χ13
χ14
χ15

FIGURE 34

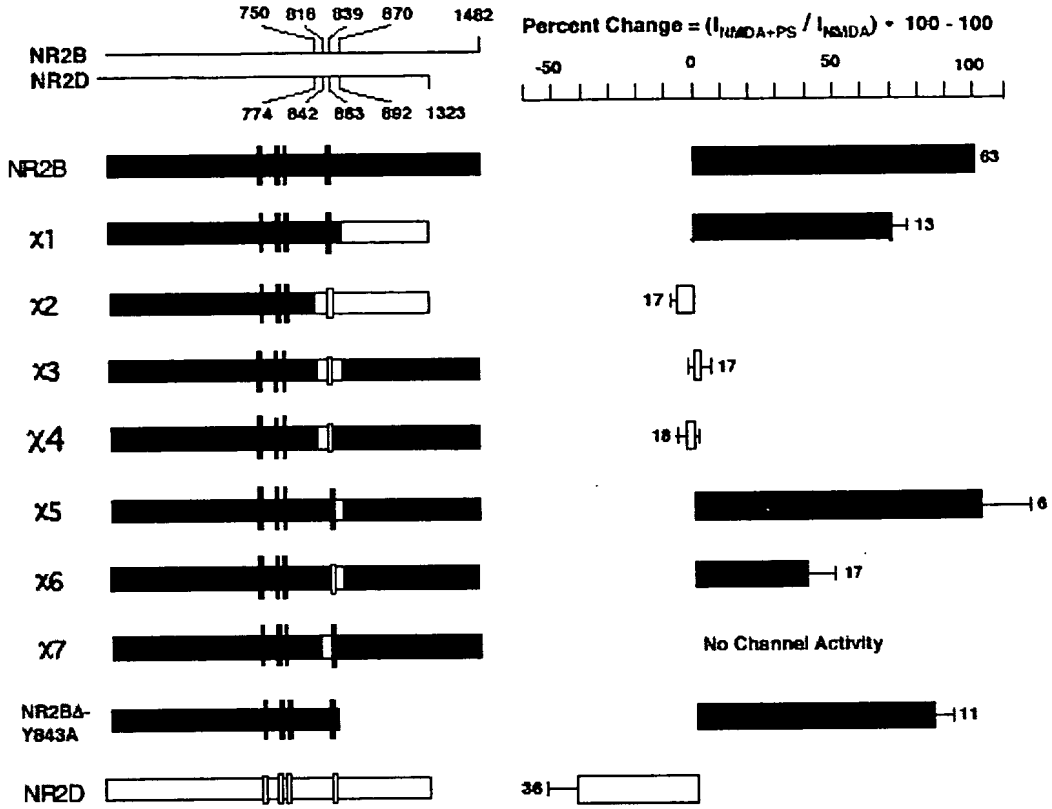
750 816 839 870 1482
NR2B
NR2D
774 842 863 892 1323
Percent Change = (I_NMDA+PS / I_NMDA) * 100 - 100
-50
0
50
100
NR2B
63
χ1
13
χ2
17
χ3
17
χ4
18
χ5
6
χ6
17
χ7
No Channel Activity
NR2BΔ-Y843A
11
NR2D
36

FIGURE 35

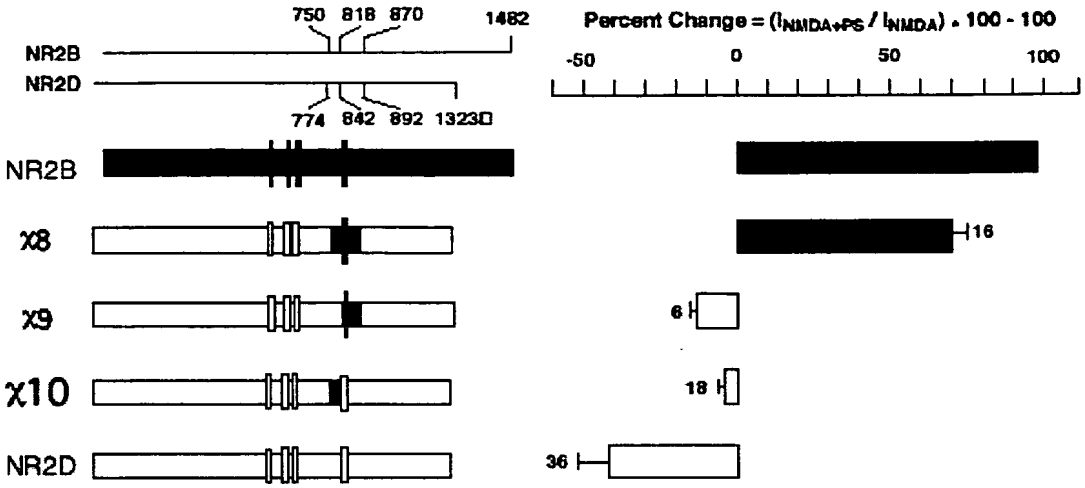
750 818 870 1482
NR2B
NR2D
774 842 892 1323
NR2B
χ8
χ9
χ10
NR2D
Percent Change = (I NMDA+PS / I NMDA) • 100 - 100
-50
0
50
100
16
6
18
36

FIGURE 36

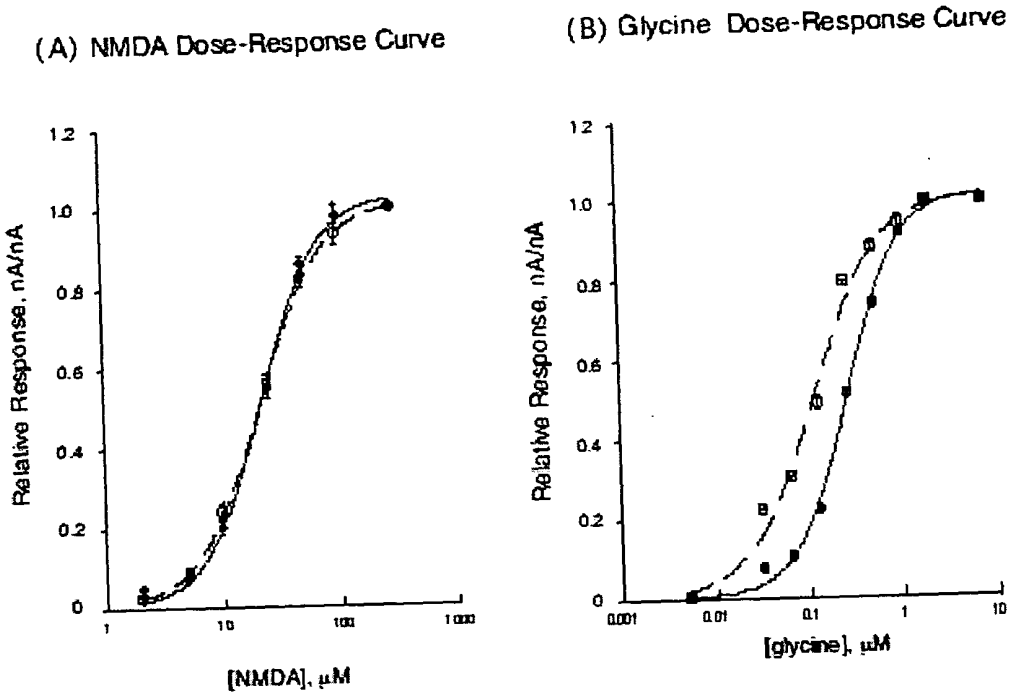
(A) NMDA Dose-Response Curve
Relative Response, nA/nA
1.2
1.0
0.8
0.6
0.4
0.2
0
1
10
100
1000
[NMDA], μM
(B) Glycine Dose-Response Curve
Relative Response, nA/nA
1.2
1.0
0.8
0.6
0.4
0.2
0
0.001
0.01
0.1
1
10
[glycine], μM

FIGURE 37

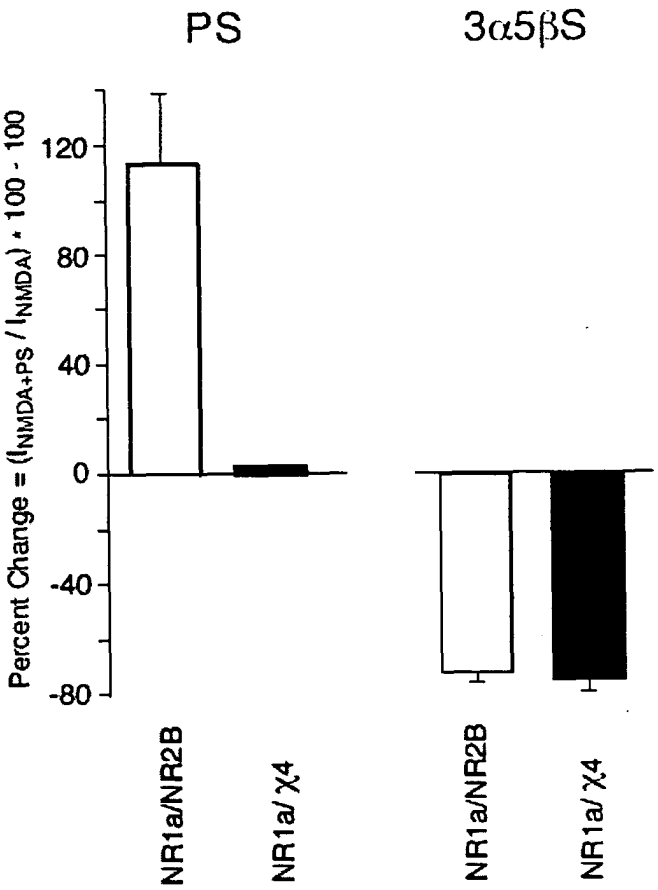
PS
3α5βS
Percent Change = (I_NMDA+PS / I_NMDA) * 100 - 100
120
80
40
0
-40
-80
NR1a/NR2B
NR1a/χ4
NR1a/NR2B
NR1a/χ4

FIGURE 38

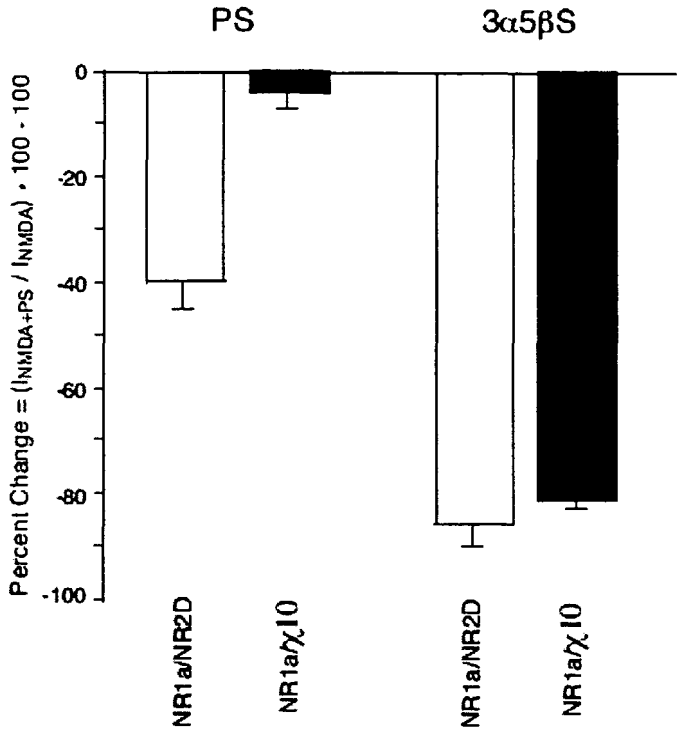
PS
3α5βS
Percent Change = (INMDA+PS / INMDA) • 100 - 100
0
-20
-40
-60
-80
-100
NR1a/NR2D
NR1a/χ10
NR1a/NR2D
NR1a/χ10

FIGURE 39

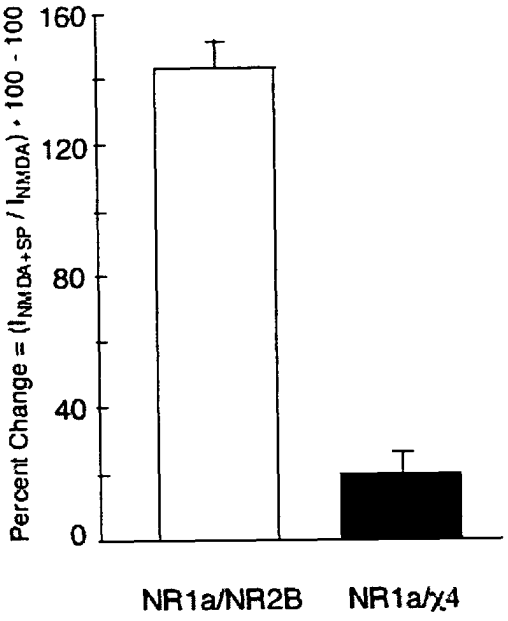
Percent Change = ($I_{NMDA+SP}$ / I_{NMDA}) * 100 - 100
160
120
80
40
0
NR1a/NR2B
NR1a/χ4

FIGURE 40

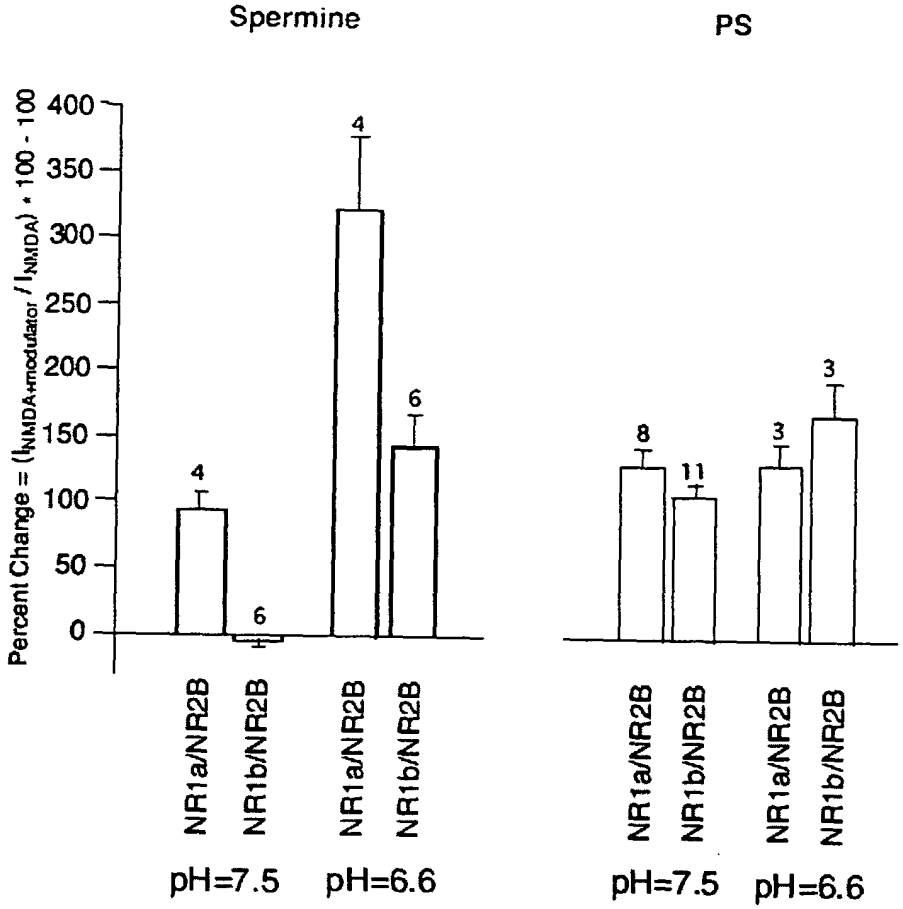
Spermine
PS
Percent Change = ($I_{NMDA+modulator}$ / I_{NMDA}) * 100 - 100
400
350
300
250
200
150
100
50
0
4
6
4
6
8
11
3
3
NR1a/NR2B
NR1b/NR2B
NR1a/NR2B
NR1b/NR2B
NR1a/NR2B
NR1b/NR2B
NR1a/NR2B
NR1b/NR2B
pH=7.5
pH=6.6
pH=7.5
pH=6.6

FIGURE 41

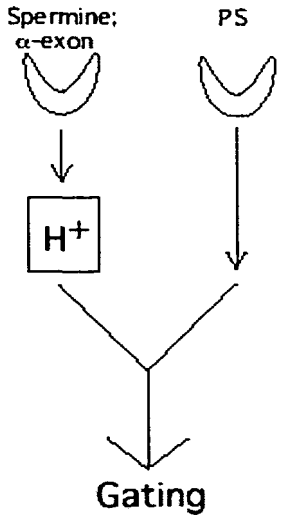

Because the potentiating effect of spermine is dependent on the proton sensor, it is plausible that the loss of the spermine effect at NR1a/χ4 containing receptors is not due to a change in the spermine-binding site, but rather a secondary phenomenon that reflects an alteration in proton sensitivity. To investigate this idea, we further characterized NR1a/χ4 receptors to investigate if proton sensitivity is altered in these receptors.

FIGURE 42

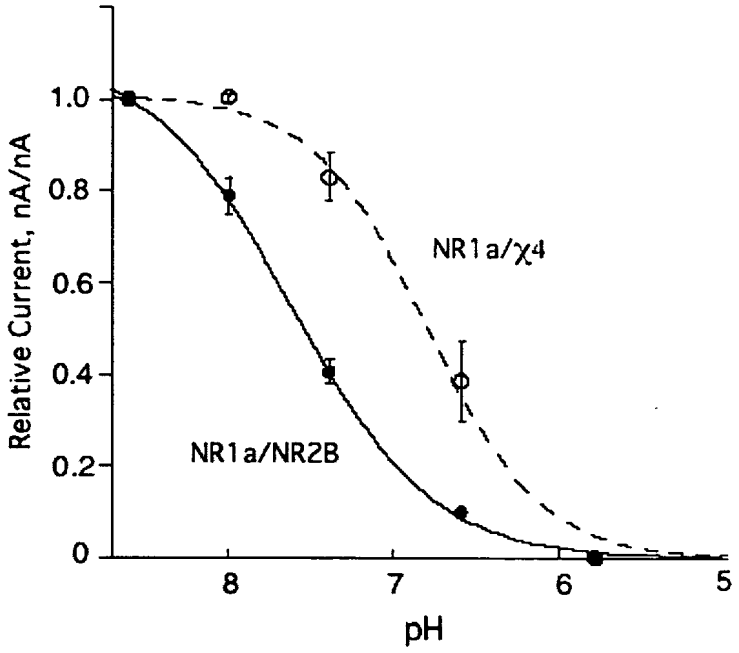
Relative Current, nA/nA
1.0
0.8
0.6
0.4
0.2
0
8
7
6
5
pH
NR1a/χ4
NR1a/NR2B

FIGURE 43

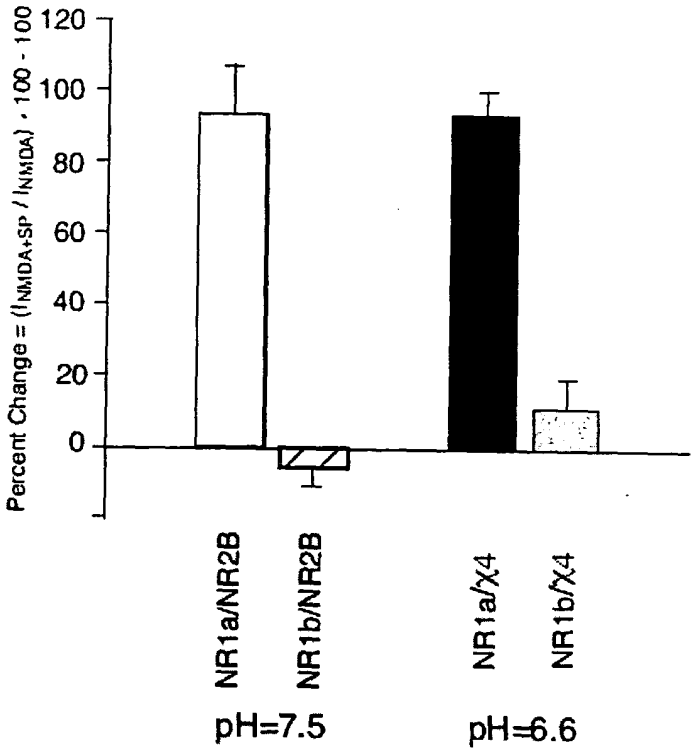
Percent Change = ($I_{NMDA+SP}$ / I_{NMDA}) * 100 - 100
120
100
80
60
40
20
0
NR1a/NR2B
NR1b/NR2B
NR1a/χ4
NR1b/χ4
pH=7.5
pH=6.6

FIGURE 44

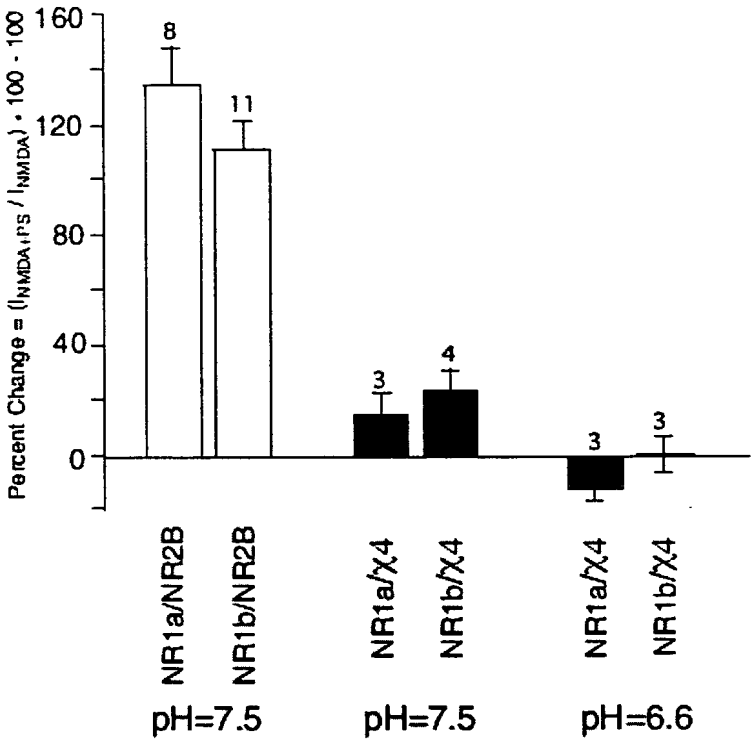
Percent Change = (I_NMDA+PS / I_NMDA) • 100 - 100
160
120
80
40
0
8
11
3
4
3
3
NR1a/NR2B
NR1b/NR2B
NR1a/χ4
NR1b/χ4
NR1a/χ4
NR1b/χ4
pH=7.5
pH=7.5
pH=6.6

FIGURE 45

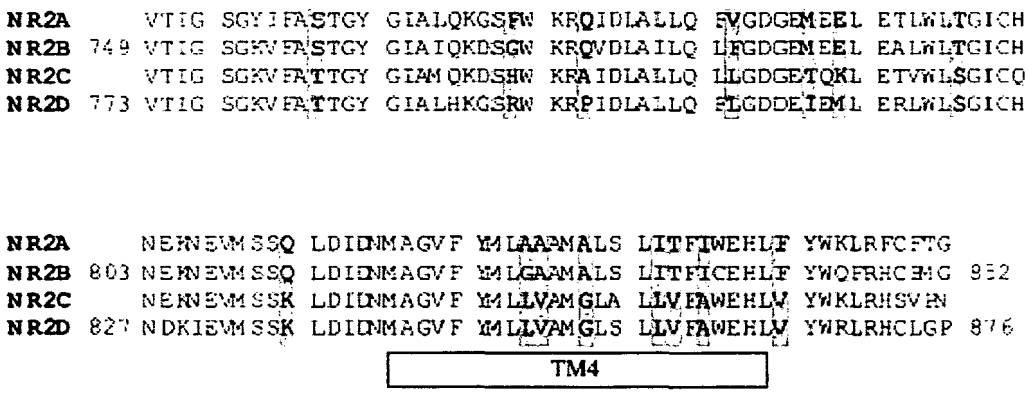
NR2A VTIG SGYIFASTGY GIALQKGSFW KRQIDLALLQ FVGDGEMEEL ETLWLTGICH
NR2B 749 VTIG SGKVFASTGY GIAIQKDSGW KRQVDLAILQ LFGDGEMEEL EALWLTGICH
NR2C VTIG SGKVFATTGY GIAMQKDSHW KRAIDLALLQ LLGDGETQKL ETVWLSGICQ
NR2D 773 VTIG SGKVFATTGY GIALHKGSRW KRPIDLALLQ FLGDDELEML ERLWLSGICH
NR2A NERNEVMSSQ LDIDNMAGVF YMLAAAMALS LITFIWEHLF YWKLRFCFTG
NR2B 803 NERNEVMSSQ LDIDNMAGVF YMLGAAMALS LITFICEHLF YWQFRHCEMG 852
NR2C NERNEVMSSK LDIDNMAGVF YMLLVAMGLA LLVFAWEHLV YWKLRHSVRN
NR2D 827 NDKIEVMSSK LDIDNMAGVF YMLLVAMGLS LLVFAWEHLV YWRLRHCLGP 876
TM4

FIGURE 46

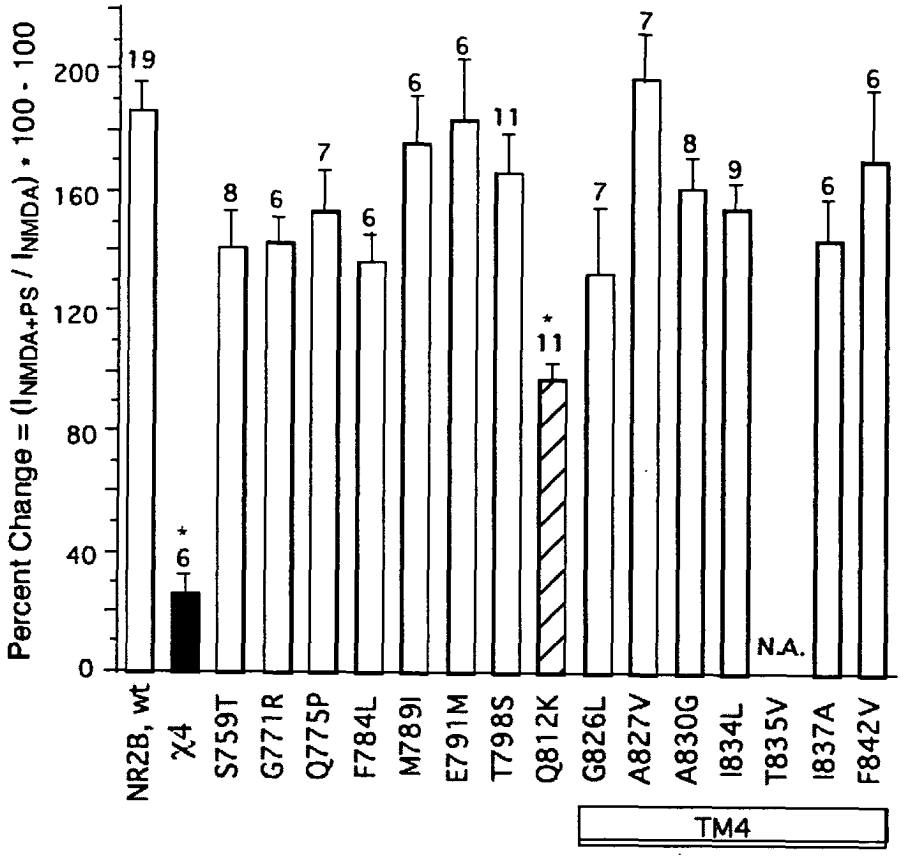
Percent Change = ($I_{NMDA+PS}$ / I_{NMDA}) • 100 - 100
0
40
80
120
160
200
19
6 *
8
6
7
6
6
6
11
11 *
7
7
8
9
N.A.
6
6
NR2B, wt
χ4
S759T
G771R
Q775P
F784L
M789I
E791M
T798S
Q812K
G826L
A827V
A830G
I834L
T835V
I837A
F842V
TM4

FIGURE 47

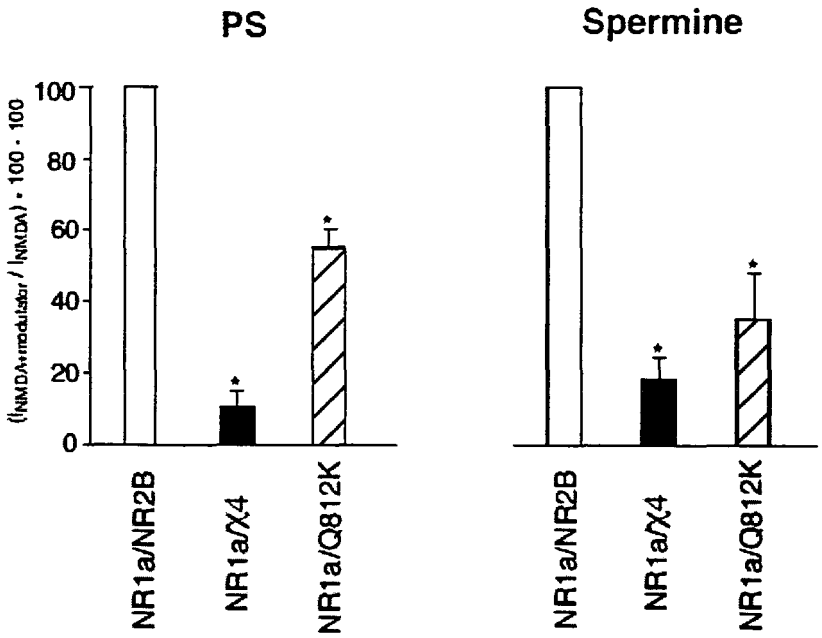
PS
Spermine
100
80
60
40
20
0
NR1a/NR2B
NR1a/χ4
NR1a/Q812K
NR1a/NR2B
NR1a/χ4
NR1a/Q812K

FIGURE 48

(A) Topology of the GluR2 subunit.

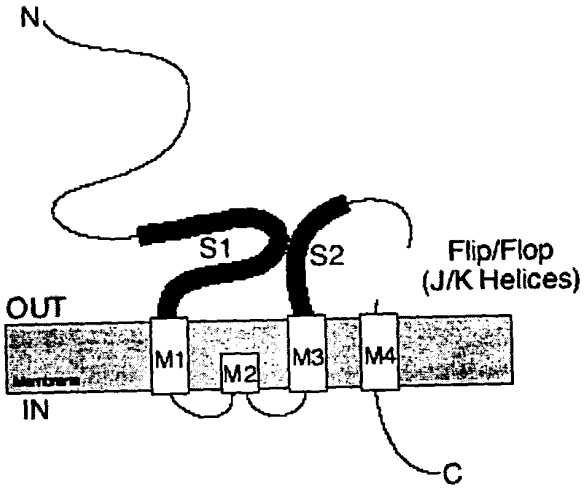

FIGURE 49

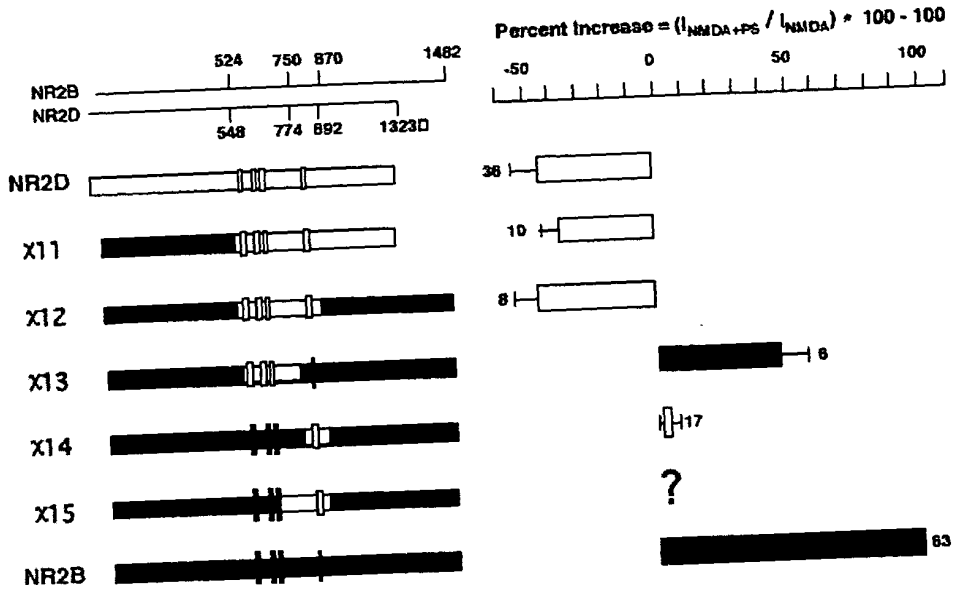
Percent increase = ($I_{NMDA+PS}$ / I_{NMDA}) * 100 - 100
-50
0
50
100
524
750
870
1482
NR2B
NR2D
548
774
892
1323D
NR2D
X11
X12
X13
X14
X15
NR2B
38
10
8
6
17
?
63